Quantifying intermolecular interactions of ionic liquids using cohesive energy densities

ROYAL SOCIETY OPEN SCIENCE

rsos.royalsocietypublishing.org

Review

Cite this article: Lovelock KRJ. 2017 Quantifying intermolecular interactions of ionic liquids using cohesive energy densities. *R. Soc. open sci.* **4**: 171223.
http://dx.doi.org/10.1098/rsos.171223

Received: 24 August 2017
Accepted: 30 October 2017

Subject Category:
Chemistry

Subject Areas:
chemical physics/materials science/physical chemistry

Keywords:
ionic liquids, cohesive energy density, intermolecular interactions

Author for correspondence:
Kevin R. J. Lovelock
e-mail: k.r.j.lovelock@reading.ac.uk

This article has been edited by the Royal Society of Chemistry, including the commissioning, peer review process and editorial aspects up to the point of acceptance.

Electronic supplementary material is available online at https://dx.doi.org/10.6084/m9.figshare.c.3937975.

ROYAL SOCIETY OF CHEMISTRY

THE ROYAL SOCIETY PUBLISHING

Quantifying intermolecular interactions of ionic liquids using cohesive energy densities

Kevin R. J. Lovelock

Department of Chemistry, University of Reading, Reading, UK

KRJL, 0000-0003-1431-269X

For ionic liquids (ILs), both the large number of possible cation + anion combinations and their ionic nature provide a unique challenge for understanding intermolecular interactions. Cohesive energy density, *ced*, is used to quantify the strength of intermolecular interactions for molecular liquids, and is determined using the enthalpy of vaporization. A critical analysis of the experimental challenges and data to obtain *ced* for ILs is provided. For ILs there are two methods to judge the strength of intermolecular interactions, due to the presence of multiple constituents in the vapour phase of ILs. Firstly, ced_{IP}, where the ionic vapour constituent is neutral ion pairs, the major constituent of the IL vapour. Secondly, ced_{C+A}, where the ionic vapour constituents are isolated ions. A ced_{IP} dataset is presented for 64 ILs. For the first time an experimental ced_{C+A}, a measure of the strength of the total intermolecular interaction for an IL, is presented. ced_{C+A} is significantly larger for ILs than *ced* for most molecular liquids, reflecting the need to break all of the relatively strong electrostatic interactions present in ILs. However, the van der Waals interactions contribute significantly to IL volatility due to the very strong electrostatic interaction in the neutral ion pair ionic vapour. An excellent linear correlation is found between ced_{IP} and the inverse of the molecular volume. A good linear correlation is found between IL ced_{IP} and IL Gordon parameter (which are dependent primarily on surface tension). *ced* values obtained through indirect methods gave similar magnitude values to ced_{IP}. These findings show that ced_{IP} is very important for understanding IL intermolecular interactions, in spite of ced_{IP} not being a measure of the total intermolecular interactions of an IL. In the outlook section, remaining challenges for understanding IL intermolecular interactions are outlined.

1. Why are intermolecular interactions of ionic liquids important?

Ionic liquids (ILs), liquids composed entirely of mobile cations and anions, are important from both an academic and an industrial standpoint [1,2]. ILs have been proposed as electrolytes, solvents for synthesis and catalysis, gas capture/storage media, lubricants, engineering fluids and in sensors [3–10].

The strength of intermolecular interactions have historically been used to understand and predict a range of properties for molecular liquids, including surface tension [11], wettability [12], the ability of a solvent to promote solute self-assembly [13,14], solubility [15] and viscosity [16–19]. All of these properties are very important for potential IL applications. For example, surface tension and wettability are key properties in understanding supercapacitors [20,21], and solubility is crucial for understanding and predicting gas separation/capture/storage [22]. Therefore, establishing links between these and other properties will give significant insight into the properties that underpin a wide range of applications.

A key property of ILs is their very low vapour pressure [23]. Hence, it is of interest to quantitatively investigate the intermolecular interactions of ILs to answer the fundamental question: do ILs have strong intermolecular interactions? In many publications it has been assumed that strong electrostatic intermolecular interactions drive the very low vapour pressures of ILs [24–27].

A pure molecular liquid contains only one constituent, the molecule; intermolecular interactions are controlled by molecule–molecule interactions. The situation is more complicated for ILs, as there are two constituents in each liquid: a cation and an anion. Both constituents will strongly influence the intermolecular interactions, making understanding intermolecular interactions of ILs much tougher than for molecular liquids. There are also many possible ILs and, therefore, many possible cation–anion combinations, providing an additional challenge to understanding intermolecular interactions of ILs.

In this article, attempts are made to find correlations for experimental measures of intermolecular interactions that hold across both molecular liquids and ILs; such correlations are particularly valuable, as these would reveal remarkable underlying similarities in intermolecular interactions. However, such correlations are expected to be very rare, given the very different chemical constituents of molecular liquids and ILs. Almost as valuable would be correlations for all ILs; such relationships that hold across ILs with a wide range of structural features are relatively rare. Lastly, family-based correlations can give significant insights into IL properties, although such correlations for relatively small groups of ILs have limited use for predicting IL properties. In this article the aim is to develop correlations for ILs using only experimental data. For certain values the required amount of experimental data does not yet exist. In such cases, quantitative correlations were not sought; however, qualitative observations were made. Data from simulations and calculations can provide an excellent complement to experimental data, and in some cases provide access to information that has not yet been experimentally measured.

In this article I use abbreviations to refer to individual ILs, instead of the IL names. The IL names, along with the relevant abbreviations, are given in the ESI, electronic supplementary material, table S1 (for cations) and electronic supplementary material, table S2 (for anions).

2. Quantifying the strength of intermolecular interactions of molecular liquids

2.1. How are the strengths of intermolecular interactions of molecular liquids quantified?

For molecular liquids the strength of intermolecular interactions is quantified using the cohesive energy density, ced_{ML}: [28,29]

$$ced_{\mathrm{ML}} = \frac{\Delta_{\mathrm{vap}}U}{V_{\mathrm{m}}} = \frac{ce}{V_{\mathrm{m}}} = \frac{\Delta_{\mathrm{vap}}H - RT}{V_{\mathrm{m}}}, \tag{2.1}$$

where $\Delta_{\mathrm{vap}}U$ is the internal energy of vaporization, i.e. the energy required to vaporize the liquid to its saturated vapour, V_{m} is the liquid molar volume ($V_{\mathrm{m}} = M/\rho$, where M = molar mass and ρ = liquid density), ce is the cohesive energy, $\Delta_{\mathrm{vap}}H$ is the enthalpy of vaporization, R is the gas constant and T is the liquid temperature. ced_{ML} is a measure of the total intermolecular cohesion per unit volume in the liquid phase, assuming negligible intermolecular interactions in the vapour [28]. Alternatively, ced_{ML} quantifies the work required to produce a hole (often called a cavity) of unit volume in the molecular liquid [30].

2.2. Conditions used for vaporization measurements for molecular liquids

Vaporization is a physical process; no chemical change to form new products occurs. There are two types of vaporization: evaporation and boiling. Evaporation is a surface process; molecules escape from the liquid surface in the gas phase, where the gas phase is not saturated with the vapour of that molecule. Boiling is a bulk process; bubbles of saturated vapour are formed by molecules in the liquid phase. In this article the focus is on evaporation. ILs have been categorized as superheated liquids, and hence, observing IL boiling is very unlikely [31].

There are two extremes of vaporization conditions. Firstly, those close to equilibrium conditions, which are preferred for obtaining thermodynamic data. These conditions are generally produced using a Knudsen effusion cell, which is a heated source containing a pinhole to allow vapour to slowly escape under effusive conditions, thus giving near-equilibrium conditions. Secondly, those far from equilibrium conditions. Evaporation occurs from the liquid–gas surface and the vapour is detected directly (with no further interactions and no chance of condensation then re-evaporation of the vaporized sample); these conditions are known as free or Langmuir evaporation. Methods for measuring $\Delta_{vap}H$ that involve a Knudsen effusion cell require higher sample temperatures (and, therefore, higher vapour pressures) than methods involving Langmuir vaporization (due to the effective smaller sample surface area available for vaporization). Higher sample temperatures also increase the probability of the chemical process of thermal decomposition (TD) occurring. For most molecular liquids the probability of vaporization, compared to the probability of TD, is sufficiently large (i.e. only sample vaporization occurs) that near-equilibrium methods are used to study vaporization, meaning that ced_{ML} can be readily determined for most molecular liquids [32].

For most molecular liquids there are negligible intermolecular interactions in the vapour, as they generally vaporize as individual isolated molecules. Therefore, ced_{ML} is a measure of the total intermolecular cohesion per unit volume in the liquid phase.

2.3. Results for the cohesive energy density for molecular liquids

$ced_{ML,298}$ values range from 195 J cm^{-3} for squalane, through 385 J cm^{-3} for acetone, 679 J cm^{-3} for ethanol, 1055 J cm^{-3} for ethanolamine and up to 2293 J cm^{-3} for water [32]. Liquid hydrocarbons can be used to explain how $\Delta_{vap}H_{298}$ and *ced* relate to intermolecular interaction strengths, and how size is vital. $\Delta_{vap}H_{298}$ increases with increasing size, from *n*-hexane ($\Delta_{vap}H_{298} = 31$ kJ mol^{-1}) to *n*-hexadecane ($\Delta_{vap}H_{298} = 81$ kJ mol^{-1}) to squalane ($\Delta_{vap}H_{298} = 105$ kJ mol^{-1}) [32,33]. However, clearly only van der Waals (vdW) interactions are added as the hydrocarbons increase in size. This fact is reflected in the $ced_{ML,298}$ values, which are in the range of approximately 190 to approximately 270 J cm^{-3} for liquid hydrocarbons [32]. These $ced_{ML,298}$ values are all very small, as expected when only vdW interactions are involved. Each liquid-phase squalane molecule forms a large number of relatively weak intermolecular interactions, all of which need to be broken in order to vaporize a squalane molecule. The increase in $\Delta_{vap}H_{298}$ from *n*-hexane to squalane is not due to stronger intermolecular interactions; there are simply more intermolecular interactions per molecule (but not per unit volume).

Many molecular liquids have significant electrostatic interactions, e.g. water, glycerol, formamide, ethanolamine. For water $\Delta_{vap}H_{298} = 44$ kJ mol^{-1} and for formamide $\Delta_{vap}H_{298} = 61$ kJ mol^{-1}, much lower than $\Delta_{vap}H_{298}$ for *n*-hexadecane and squalene [32,33]. However, water and formamide are significantly smaller than *n*-hexadecane and squalene [32,33]. Therefore, water and formamide give much larger ced_{ML} values than for hydrocarbons [32], demonstrating that the intermolecular interactions in molecular liquids that have significant electrostatic interactions are much stronger than in hydrocarbons.

3. How the cohesive energy density relates to other properties for molecular liquids

Given the interest in correlating *ced* with other properties, it is vital to know how ced_{ML} values correlate to other liquid-phase properties.

3.1. Surface tension

Surface tension, γ, is a key parameter for colloid science and engineering [14]. Surface tension represents the energy required to separate a bulk liquid to create two new liquid–gas surfaces, i.e. the energy per

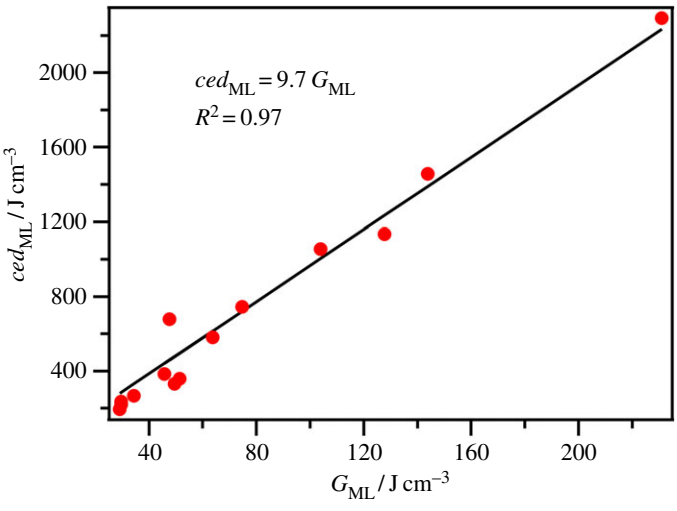

Figure 1. ced_{ML} versus G_{ML} for select molecular liquids.

surface area. Forming such surfaces requires breaking bulk intermolecular interactions [34–38]. In 1896, Stefan proposed that the work necessary to bring a molecule from the interior of the liquid to the surface is half that needed to vaporize it [37]. For samples that will thermally decompose before vaporization occurs, i.e. involatile liquids and polymers, the Gordon parameter, G [11], has been used as a substitute for *ced*: [14,39]

$$G = \frac{\gamma}{V_{mol}^{1/3}}, \tag{3.1}$$

where γ is the surface tension and V_{mol} is the molecular volume ($V_{mol} = V_m/N_a$, where N_a = Avogadro's number). Owing to the possible influence of the surface structure on γ and therefore G, *ced* is generally preferred over G for investigating intermolecular interactions. However, for non-volatile samples G is easier to measure than $\Delta_{vap}H$. A very good linear correlation between ced_{ML} and G_{ML} is observed for a small selection of molecular liquids (figure 1).

3.2. Liquids as solvents for self-assembly

Solute self-assembly in solvents is vital in many areas, including in nature (in particular in water), drug delivery, inorganic materials and many more [13,14]. Until recently only approximately 20 solvents were known to promote self-assembly [40], although more have been found recently [41]. In particular, many protic ILs and a number of aprotic ILs have been found to promote self-assembly [40,42,43]. For ILs there are essentially two categories of cation: aprotic ILs are formed by transfer of an alkyl chain from e.g. an alkylchloride to a base, whereas protic ILs are formed by transfer of a proton from a Brønsted acid to a Brønsted base [44,45]. *ced* can be considered to represent the tightness or structuredness of liquids as caused by intermolecular interactions [30]. It has been demonstrated that structured liquids support self-assembly of amphiphilic molecules, due to the large *ced* [13,41]. Structural properties of liquids acting as solvents can be categorized by stiffness, as measured by the work that must be expended to create a hole in the liquid, as expressed by the liquid *ced* [46]. Evans has proposed that liquids with G (as a substitute for *ced*) $> \sim 110\ J\ cm^{-3}$ tend to promote aggregation of amphiphilic molecules, i.e. G and *ced* can be used as measures of a solvent's solvophobic strength [13,14,47].

3.3. Solubility

Predicting the solubilities/miscibilities of gases/solvents in/with ILs is of vital importance [4,22], and a general prediction scheme would be of great use. Hildebrand showed that for non-polar liquids:

$$\delta_H = ced^{0.5}, \tag{3.2}$$

where δ_H is the Hildebrand solubility parameter [28]. δ_H is typically small for non-polar solvents and large for polar solvents [48]. If δ_H is similar for solvent and solute then it is predicted that solvation will occur, as similar strength interactions will be broken and formed. δ_H predicts solubility well for non-polar

and slightly polar molecules, where vdW interactions are dominant. For systems where electrostatic interactions (e.g. polar liquids) are important, a one-component parameter such as δ_H does not represent the system sufficiently, and more components are required to explain solubility [15,49]. Hansen solubility parameters comprise: polar, non-polar and hydrogen bonding, and they can be estimated using indirect methods.

Activity coefficients give a measure of interactions between solute and solvent, and are used to obtain $\delta_{H,indirect}$ for liquids (δ_H values for ILs determined from activity coefficients are referred to in this article as $\delta_{H,indirect}$, to differentiate between δ_H values obtained from *ced*). Activity coefficients at infinite dilution for solutes in ILs have been measured using inverse gas chromatography, and $\delta_{H,indirect}$ was obtained (*ced* values for ILs determined from these $\delta_{H,indirect}$ values are referred to in this article as $ced_{indirect}$) [50].

3.4. Viscosity

Viscosity is a key variable in process design, e.g. mixing, separation, lubrication. Viscous flow is often modelled by the activated jumping of a molecule from an initial configuration to a second position, separated by an intermediate activated state [18]. Eyring and co-workers postulated that the activated state of the molecule requires a larger volume than the initial state. As this larger volume requires hole creation in the liquid, the activation energy for viscous flow, $E_{a,vis}$, should be a fraction of $\Delta_{vap}U$:

$$\Delta_{vap}U = ce = ced.V_m = C.E_{a,vis}, \tag{3.3}$$

where C is a constant for 'normal' liquids. For non-spherical molecules (e.g. hexane and acetone) $C \approx 4$; for small spherical molecules (e.g. CCl_4 and cyclohexane) $C \approx 3$. For both liquid metals and molten salts the unit of flow was considered to be important; to obtain a satisfactory linear correlation between $\Delta_{vap}U$ and $E_{a,vis}$, atomic/ionic radii were included in correlations [19,51]. A further possible complication is that the relationship between viscosity and temperature does not follow Arrhenius-like behaviour just above the glass transition temperature for all ILs (i.e. many ILs are fragile liquids), leading to possible errors in measured $E_{a,vis}$ for ILs [52].

δ_H, and therefore *ced*, can also be determined using measurements of intrinsic viscosity (*ced* values for ILs are again referred to as $ced_{indirect}$). The viscosity of a dilute solution of a solute (e.g. a polymer) is a maximum in the 'best' solvent, i.e. the solution where cohesion properties of solvent and solute are comparable [53].

3.5. Internal pressure

The internal pressure of a liquid, P_{int}, is another property that can be used to quantify intermolecular interactions. ced_{ML} depends on breaking all intermolecular interactions. P_{int} for molecular liquids depends on small isothermal expansion; intermolecular distances increase slightly so not all intermolecular interactions are broken. The ratio:

$$r = \frac{P_{int}}{ced}, \tag{3.4}$$

is the standard method to compare P_{int} to *ced*. r can be used to categorize solvents. Liquids where $r > 1.2$ are labelled as loose, e.g. fluorocarbons, triethylamine (repulsive interactions are relatively large) [54]. Liquids with $r < 0.8$ are collectively labelled as associated/tight/stiff liquids, e.g. water, ethanolamine (attractive interactions are strong) [54]. Liquids with $r \sim 1$ are non-polar liquids, e.g. hydrocarbons, diethyl ether, toluene [28,54]. This ratio also highlights that P_{int} and *ced* have the same units, generally MPa or J cm^{-3}.

4. Measuring the cohesive energy density for ionic liquids: overcoming the challenges

There are two major experimental challenges for obtaining *ced* for ILs (V_m can be readily measured with good accuracy for ILs [55]). Firstly, measuring the amount of IL ionic vapour at different temperatures to obtain $\Delta_{vap}H$. The inherently low vapour pressure of ILs makes these measurements difficult. For $[C_2C_1Im][NTf_2]$ at $T = 298$ K the vapour pressure can be estimated as approximately 10^{-9} Pa [56], a much lower value than the expected detection limits for any apparatus used for studying vaporization of molecular liquids. Secondly, the ionic vapour composition needs to be known under the conditions

for which $\Delta_{vap}H$ is measured (ionic vapour refers only to the vaporization of intact IL) [57], so that the nature of the intermolecular interactions broken is known.

4.1. Ionic liquids can be distilled

For many years, it was assumed that IL TD followed by vaporization of the non-ionic TD products occurred more readily than IL vaporization of intact ionic vapour. Hence, it was assumed that ILs had no detectable vapour pressure [58–60].

Since 2005 it has become accepted that ILs can be vaporized, in contradiction of previous assumptions. The major evidence for IL vaporization was their successful distillation, i.e. the physical process of IL vaporization, followed by condensation of the same species that was vaporized. Bulk-scale distillation of intact IL has been achieved for 1,3-dialkylimidazolium-, 1,1-dialkylpyrrolidinium- and tetraalkylammonium-based ILs at a temperature range of 475 to 575 K [61–63]. Most of the focus has been on $[NTf_2]^-$-based ILs, which have the required combination of relatively good thermal stability and relatively high volatility [31,64,65]. Aprotic ILs are the focus of this article, as very few vaporization studies of protic ILs have been published, in particular on identification of the vapour phase species [66–69].

4.2. The vapour phase composition of ionic liquids: the ionic vapour

In the seminal 2006 *Nature* article demonstrating distillation of ILs, it was speculated that IL vaporization occurred as isolated ions or as ion aggregates [61,70]. Additionally, a chemical process of IL transfer could not be ruled out.

4.2.1. The ionic vapour: intact ions in the vapour phase

For a wide range of ILs using positive mode mass spectrometry (MS) (with electron ionization, field ionization or photoionization) the parent cation, $[C]^+$ [57,63,66,71–89], has been detected intact in the vapour phase (at $350\,K < T < 700\,K$). In addition, the parent anion, $[A]^-$ [66,83,85], has been detected intact in the vapour phase using negative mode MS (with electron ionization or photoionization). The cations investigated include $[C_nC_1Im]^+$, $[C_nC_1Pyrr]^+$, $[C_nPy]^+$, tetraalkylphosphonium and alkylisouronium; the anions investigated include $[NTf_2]^-$, $[PF_6]^-$ and $[TfO]^-$. If IL TD products were vaporizing instead of intact IL vaporizing, one would not expect to detect intact parent cations and parent anions. For example, electron ionization MS of the products of heating $[C_nC_1Im][A]$ ILs (A^- = halide ion) found non-ionic TD products such as 1-methylimidazole and alkyl halides [77,90]. Therefore, intact ionic has definitely been detected for a wide range of ILs. Leading on from this detection of intact parent ions in the mass spectra, there are two key questions to be answered about the ionic vapour.

4.2.2. The ionic vapour is composed of neutral species, not isolated ions

For a wide range of ionic vapours, when the MS ionization source, e.g. electrons, was turned off, no ions were detected; it was concluded that the vapour phase of ILs is composed primarily of neutral species, not isolated ions [57,63,66,71–77]. More recently, using a specialist Knudsen effusion cell to produce the vapour of $[C_2C_1Im][NTf_2]$ and electric fields to extract any overall charged ions in the vapour phase, $[C]^+$, $[C_2A]^+$, $[A]^-$ and $[CA_2]^-$ were detected [87,91]. However, the amount of ions in the vapour phase was approximately 10^8 to 10^{11} times lower than the amount of CA ion pairs [56], demonstrating the lack of significant amounts of overall charged ions in the vapour phase for $[C_2C_1Im][NTf_2]$. Lastly, the intact molecular ion, $[CA]^{+\bullet} = [C_4C_1ImC(CN)_3]^{+\bullet}$, was detected for $[C_4C_1Im][C(CN)_3]$ using both field ionization and photoionization at m/z 229 [78,82], demonstrating that the lack of $[CA]^{+\bullet}$ detected for other ILs should not be taken as an indication of the lack of neutral vapour prior to ionization. Overall, these findings show that the vapours of the ILs studied to date are composed predominantly of neutral species.

4.2.3. The ionic vapour is composed of one cation and one anion, not larger clusters

No higher mass clusters of the form $[C_mA_{m-1}]^+$ (where $m \geq 2$) have been observed after either electron ionization or photoionization of a wide range of ILs [57,63,66,71–77,79–82]. It has been suggested that for electron ionization too much excess energy is deposited into the ionic vapour, which will lead to the break-up of higher mass clusters such as C_3A_3 [92] (if such clusters are present in the ionic vapour).

Vaporization as C_mA_m where $m \geq 2$ occurs for alkali halides such as LiCl, and after electron ionization cluster ions such as $[Li_3Cl_2]^+$ were detected [93]. This finding suggests that electron ionization MS may be able to detect higher mass clusters such as C_3A_3 (if such clusters are present in the vapour phase). For $[C_4C_1Im][C(CN)_3]$ the intact molecular ion, $[CA]^{+\bullet}$, has been detected using field ionization and photoionization [78,82], but no higher mass clusters were detected up to m/z 600; no $[C_2A]^+$ (m/z 368), $[C_2A_2]^{+\bullet}$ (m/z 458) or $[C_3A_2]^+$ (m/z 597) were observed [82]. $[CA]^{+\bullet}$ is expected to have a significantly weaker intermolecular cation–radical interaction than the cation–anion intermolecular interactions in $[C_2A]^+$. Therefore, observation of $[CA]^{+\bullet}$ but not $[C_2A]^+$, $[C_2A_2]^{+\bullet}$ or $[C_3A_2]^+$ shows that $[C_2A]^+$, C_2A_2 or $[C_3A_2]^+$ were not present in significant concentrations in the ionic vapour.

Reactions of the form $[C]^+ + (\text{ionic vapour}) \rightarrow (\text{product ions})$ and $[A]^- + (\text{ionic vapour}) \rightarrow (\text{product ions})$ were carried out for $[C_6C_1Im][NTf_2]$, $[P_{6,6,6,14}][TfO]$ and $[C_4C_1Pyrr][NTf_2]$ [66]. $[C_2A]^+$ and $[CA_2]^-$ were detected for the respective reactions, as would be expected if the ionic vapour was composed of CA neutral ion pairs. However, larger cluster ions, e.g. $[C_3A_2]^+$, were not detected, demonstrating that the ionic vapour was not composed of C_2A_2 clusters, or any larger clusters.

Two ionization mechanisms have been proposed for ILs, demonstrated below for photoionization: dissociative ionization [71] (mechanism 1) and CA neutral ion pair dissociation [83] (mechanism 2):

$$CA + h\nu \rightarrow [CA]^{+\bullet} \rightarrow [C]^+ + A^\bullet \qquad \text{(mechanism 1)}$$

$$CA + h\nu \rightarrow [C]^+ + [A]^- \qquad \text{(mechanism 2).}$$

It should also be noted that one dicationic IL has successfully been vaporized. The ionic vapour was shown to consist of CA_2 neutral ion triplets [94,95].

4.2.4. The ionic vapour under equilibrium conditions

Most of the studies described in §§4.2.1 to 4.2.3 were performed under Langmuir vaporization conditions (for ILs with a wide range of different structures), i.e. not under equilibrium conditions [57,63,66,71–85]. Therefore, it is very important to highlight those studies that were performed under near-equilibrium conditions. A combination of a Knudsen effusion cell with a small orifice with MS detection has been used by a number of research groups to study the ionic vapour of $[C_nC_1Im][NTf_2]$ [86–89,91]. All evidence is in agreement with that given already in §4, demonstrating that the equilibrium ionic vapour for $[C_nC_1Im][NTf_2]$ ILs is composed of neutral ion pairs. At present ILs with other anions have not been successfully vaporized using a Knudsen effusion cell, e.g. $[C_nC_1Im][PF_6]$ ILs thermally decomposed in a Knudsen effusion cell [96].

When flash heating an IL/acetonitrile mixture, i.e. heating from room temperature to very high temperature very rapidly (nearly instantaneously to incandescence, expected to give $T > 1000$ K), larger clusters of the type $[C_2A]^+$ and $[CA_2]^-$ were detected using MS [92]. It was suggested that these clusters were formed via gas-phase decomposition of neutral clusters, e.g. C_2A_2 [92]. However, such conditions are very far from equilibrium conditions and $\Delta_{vap}H$ was not measured in this study; the composition of the ionic vapour at such temperatures does not appear to be relevant for $\Delta_{vap}H$ measurements.

4.2.5. Investigating the ionic vapour using simulations and calculations

Simulations and calculations in the temperature range relevant to IL experimental vaporization studies ($360\,K < T < 630\,K$, see electronic supplementary material, table S3) have shown mainly isolated, neutral ion pairs in the ionic vapour [97,98]. Simulations at temperatures well above those at which vaporization experiments have been carried out (i.e. $T > 800$ K) have suggested the presence of higher mass clusters [97,99–102]. In addition, below T approximately 350 K calculations found that the major constituent of the ionic vapour was C_4A_4 for $[C_4C_1Im][CF_3SO_3]$ [97]. Measurements of $\Delta_{vap}H_T$ have been made at a wide variety of different T, ranging from 370 to 625 K [57]. As will be explained in §4.4.2, extrapolations of $\Delta_{vap}H_T$ are regularly made to T values for below those at which $\Delta_{vap}H_T$ was measured, especially to $T = 298$ K. An important assumption for such extrapolations is that the ionic vapour remains the same at the target T as that T at which $\Delta_{vap}H_T$ was measured. For example, to be confident in an extrapolation to $T = 298$ K, one needs to know what the ionic vapour composition is at 298 K. At present, the best effort to experimentally determine the ionic vapour composition near $T = 298$ K is at $T = 340$ K for $[C_2C_1Im][NTf_2]$, which suggested that the ionic vapour was composed of neutral ion pairs [57], although checking for C_4A_4 was not possible on the apparatus used due to m/z 1285 for $[C_4A_3]^+$ being beyond the detector m/z range. Thus, there is currently no experimental evidence to confirm or deny the presence of clusters larger than ion pairs in the vapour of ILs at $T = 298$ K.

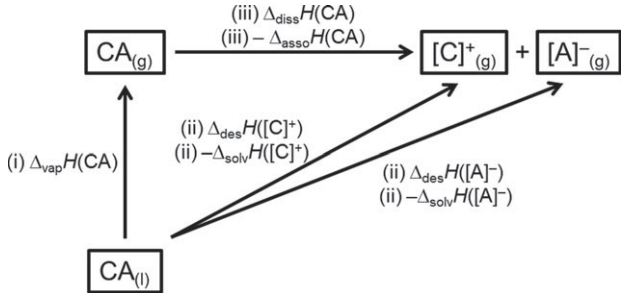

Scheme 1. Extended Born–Fajans–Haber cycle for transformations of an ionic liquid in terms of enthalpies. Adapted from Preiss *et al.* [103].

4.2.6. Isolated ions in the ionic vapour

It has previously been stated that the enthalpy of desorption for an IL ion pair from the bulk IL, $\Delta_{des}H$(total), cannot be measured directly, which were reasonable statements at the time, given the very challenging nature of these experiments [103,104]. As noted in §4.2.2, for $[C_2C_1Im][NTf_2]$ high temperature-capable thermal ion emission MS has been used to detect ionic vapour species with net overall charge, i.e. very small quantities of isolated $[C]^+$ and $[A]^-$ ions have been detected in the ionic vapour [87,91]. From measurements of the amount of $[C]^+$ and $[A]^-$ ions in the equilibrium ionic vapour at different temperatures the enthalpy of cation desorption from the bulk IL, $\Delta_{des}H([C]^+)$ and the enthalpy of anion desorption from the bulk IL, $\Delta_{des}H([A]^-)$ have been determined, respectively [87,91]. Therefore, experimental values for $\Delta_{des}H([C]^+)$ and $\Delta_{des}H([A]^-)$ (and therefore, $\Delta_{solv}H([C]^+)$ and $\Delta_{solv}H([A]^-)$) have now be obtained [87,91].

4.2.7. Summary

All evidence leads to the conclusion that vaporization occurs primarily as CA neutral ion pairs (i.e. no net overall charge), and vaporization as C_mA_m where $m \geq 2$ does not occur to any significant level. There are very small amounts of isolated ions in the ionic vapour (i.e. species with net overall charge). There are open questions about the nature of the equilibrium ionic vapour composition for many ILs and the ionic vapour composition at room temperature; these will be outlined in §9.

4.3. Two different measures of cohesive energy density for ionic liquids

The molecular unit for an IL is made up of one cation and one anion, i.e. the molar mass of an IL is always taken from one cation and one anion, M_{IP}. Much research has been carried out into the occurrence of ion pairs in bulk ILs; the general consensus is that long-lived ion pairs do not exist as individual entities in the bulk of ILs, at least at room temperature [105]. Therefore, the molecular units in the bulk IL (i.e. isolated ions, see §4.2) and in the ionic vapour (i.e. isolated neutral ion pairs) are different. As the bulk IL is made up of individual ions, the cation–anion interaction present in the neutral ion pair ionic vapour is deemed as intermolecular, as has been concluded elsewhere [104]. This judgement leads to two different versions of *ced* for ILs, here labelled ced_{IP} (*ced* when the ionic vapour is a neutral ion pair CA) and ced_{C+A} (*ced* when the ionic vapour is isolated ions, $[C]^+$ and $[A]^-$).

The traditional equation for *ced* (see equation (2.1)) can be used for ILs:

$$ced_{IP} = \frac{\Delta_{vap}H - RT}{V_m}, \tag{4.1}$$

where IP denotes ion pair, as the ionic vapour is a neutral ion pair (scheme 1, step (i)) and V_m is the IL molar volume ($V_m = M_{IP}/\rho$, where M_{IP} = IL molar mass and ρ = IL density). Therefore, ced_{IP} of an IL can readily be obtained using $\Delta_{vap}H$ (scheme 2, step (i)).

The energy to form isolated cations and isolated anions in the gas phase from the liquid phase can be obtained from $\Delta_{des}H$(total) (scheme 1, step (ii)). $\Delta_{des}H(\text{total}) = -\Delta_{solv}H(\text{total})$, where $\Delta_{solv}H$(total) represents the sum of the enthalpy of cation solvation from the vapour phase into the bulk IL, $\Delta_{solv}H([C]^+)$, and the enthalpy of anion solvation from the vapour phase into the bulk IL, $\Delta_{solv}H([A]^-)$.

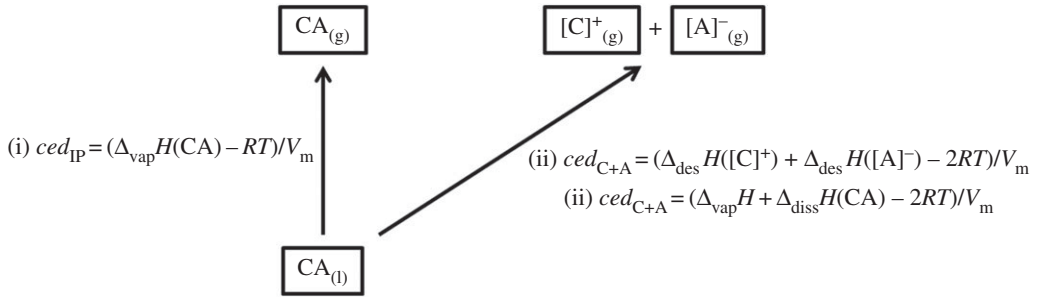

Scheme 2. Transformations of an ionic liquid in terms of *ced*.

ced_{C+A} can be obtained by measuring $\Delta_{des}H(\text{total})$ (scheme 2, step (ii)).

$$\Delta_{des}H(\text{total}) = \Delta_{des}H([C]^+) + \Delta_{des}H([A]^-) \tag{4.2}$$

$$ced_{C+A} = \frac{\Delta_{des}H(\text{total}) - 2RT}{V_m}. \tag{4.3}$$

Isolated gas-phase cations and anions can also be formed by vaporizing a neutral ion pair (scheme 1, step (i)) and then breaking the cation–anion intermolecular interaction (scheme 1, step (iii)). Therefore, ced_{C+A} can be obtained by measuring $\Delta_{vap}H$ and the enthalpy of vapour phase neutral ion pair dissociation, $\Delta_{diss}H(CA)$ (scheme 1, step (ii)).

$$\Delta_{des}H(\text{total}) = \Delta_{vap}H + \Delta_{diss}H(CA) \tag{4.4}$$

$$ced_{C+A} = \frac{\Delta_{vap}H + \Delta_{diss}H(CA) - 2RT}{V_m}. \tag{4.5}$$

As there are significant intermolecular interactions in the vapour, ced_{IP} does not capture all liquid-phase intermolecular interactions for an IL, i.e. ced_{IP} is not a measure of the total intermolecular cohesion per unit volume in the IL. ced_{C+A} captures all liquid-phase intermolecular interactions for an IL, i.e. ced_{C+A} is a measure of the total intermolecular cohesion per unit volume in the IL.

4.4. Problems caused by the low vapour pressure of ionic liquids

4.4.1. Monitoring the amount of ionic liquid vaporized

Accurately detecting the very small amounts of IL vaporization with respect to temperature is very challenging experimentally, especially with apparatus developed for molecular liquids. Hence, methods have been developed to measure IL vaporization at the temperatures required. Improvements in the sensitivity of vaporization detection mean that measurements have been made at increasingly lower temperature; therefore, TD is expected to be less of a complication for measurements made at lower temperatures.

There are broadly two methods to monitor the amount of IL vaporized with respect to temperature (scheme 3). Method 1: measure the amount of IL lost on vaporization from the liquid phase. Techniques that can be used to monitor the mass lost as the IL vaporizes include Knudsen effusion mass loss [56,88], calorimetry [106,107], thermogravimetric analysis (TGA) [31,64,65,108–116] and transpiration [117]. Method 2: measure the amount of ionic vapour in the gas phase produced by IL vaporization. Within Method 2, there are two approaches to determine the amount of ionic vapour in the gas phase: (a) measure the amount of ionic vapour in the gas phase (temperature-programmed MS (TPMS) [57,63,71–77,86], temperature-programmed photoelectron spectroscopy (TPPES) [80], UV absorption spectroscopy [118]), (b) measure the amount of ionic vapour that has condensed from the gas phase onto a solid surface (quartz crystal microbalance (QCM) [96,110–112,114–116,119–136], magnetic suspension balance (MSB) [31]).

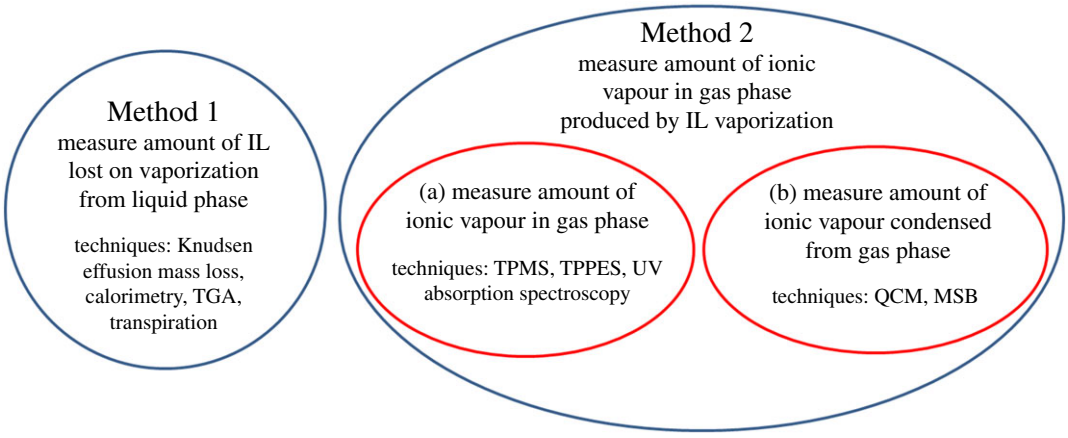

Scheme 3. The two methods used to monitor the amount of IL vaporized with respect to temperature. Within Method 2, there are two approaches to determine the amount of ionic vapour in the gas phase. TGA, thermogravimetric analysis; TPMS, temperature-programmed mass spectrometry; TPPES, temperature-programmed photoelectron spectroscopy; QCM, quartz crystal microbalance; MSB, magnetic suspension balance.

4.4.2. Comparing measured $\Delta_{vap}H_T$: adjusting $\Delta_{vap}H_T$ to a common temperature

Measurements of $\Delta_{vap}H_T$ have been made at a wide range of T, from 370 to 625 K [57]. To make valid comparisons of $\Delta_{vap}H_T$ a common T is needed. To obtain $\Delta_{vap}H_T$ at a constant T (usually $T = 298$ K) an extrapolation is required from the measurement T to the constant T used for $\Delta_{vap}H_T$ comparisons. Such an extrapolation requires knowledge of the heat capacity at constant pressure, $\Delta^g_lC_p$, between the IL in the vapour and liquid phases, over the T range of interest. It has been noted that this extrapolation was a major source of discrepancies for published $\Delta_{vap}H_{298}$ values for ILs [111]. For ILs, the liquid phase heat capacities can be readily measured [137]. However, the gas-phase heat capacities have not been measured to date, and have been judged to be impossible to measure [111]. Thus, different methods of obtaining $\Delta^g_lC_p$, have been proposed. However, the variety of different methods and $\Delta^g_lC_p$ values used means that a summation is required.

Quantum mechanical and statistical thermodynamic calculations on ionic vapour neutral ion pairs have been used to obtain the gas-phase heat capacity for $[C_nC_1Im][PF_6]$ [138]. Based upon this value, a value for $\Delta^g_lC_p$ in the region of $-100\,J\,K^{-1}\,mol^{-1}$ has been used for a wide variety of ILs [56,57,63,71–73,75,77,108,117,118,122,123,131,134,136]. Quantum mechanical and statistical thermodynamic calculations on ionic vapour neutral ion pairs have been used to obtain gas-phase heat capacities for $[C_nC_1Im][NTf_2]$ ($n = 2$, 4, 6, 8) [139]. Correlations developed from these values have then been used to obtain $\Delta^g_lC_p$ for $[C_nC_mIm][NTf_2]$ ILs, ranging from $\Delta^g_lC_p = -112\,J\,K^{-1}\,mol^{-1}$ for $[C_2C_1Im][NTf_2]$ to $\Delta^g_lC_p = -203\,J\,K^{-1}\,mol^{-1}$ for $[C_{10}C_{10}Im][NTf_2]$ [129,130,132,133,135]. Clearly, there are very large and unsatisfactory discrepancies between these $\Delta^g_lC_p$ values and the widely used $\Delta^g_lC_p = -100\,J\,K^{-1}\,mol^{-1}$ value; these differences can lead to significant variation in $\Delta_{vap}H$ values, up to 20 kJ mol^{-1} for ILs with long alkyl chains [111].

In 2013, Verevkin *et al.* [111] analysed their $\Delta_{vap}H$ data for $[C_nC_1Im][NTf_2]$ ($n = 1$–18) measured using two different techniques, TGA and QCM. As the T at which the $\Delta_{vap}H_T$ data were recorded using the two techniques were different by approximately 150 K, values for $\Delta^g_lC_p$ could be indirectly determined using this experimental $\Delta_{vap}H_T$ data. $\Delta^g_lC_p$ was found to range from $\Delta^g_lC_p = -56\,J\,K^{-1}\,mol^{-1}$ for $n = 2$ to $\Delta^g_lC_p = -170\,J\,K^{-1}\,mol^{-1}$ for $n = 16$. This procedure using variable $-T\,\Delta_{vap}H_T$ data has since been applied to more ILs, although to date they have all been for ILs with an $[NTf_2]^-$ anion [88,106,114–116]; for example, $\Delta^g_lC_p = -67\,J\,K^{-1}\,mol^{-1}$ for $n = 4$ has been found, in excellent agreement with the findings of Verevkin and co-workers [88]. Overall, $\Delta^g_lC_p$ has generally been found to be in the range of -40 to $-120\,J\,K^{-1}\,mol^{-1}$ for ILs with relatively few CH_2 groups, whereas for ILs with relatively large amounts of CH_2 groups $\Delta^g_lC_p$ has generally been found to be in the range of -120 to $-200\,J\,K^{-1}\,mol^{-1}$. All groups have found a chain length dependence of $\Delta^g_lC_p$. Most recently, $\Delta^g_lC_p = -62\,J\,K^{-1}\,mol^{-1}$ has been proposed using a combination of experimental $\Delta_{vap}H_T$ data measured at different T and educated guesses [140]. When compared to $\Delta^g_lC_p$ derived from both methods explained above (calculations and indirectly from experimental data), $\Delta^g_lC_p = -62\,J\,K^{-1}\,mol^{-1}$ appears too small for ILs with relatively large numbers of CH_2 groups, e.g. $[C_{12}C_1Im][NTf_2]$ and $[C_6C_6Im][NTf_2]$.

Overall, there are two possible options for obtaining $\Delta_{vap}H_T$ at a common T. Firstly, use $\Delta^g_lC_p$ values defined in the literature where available, and otherwise use a constant, IL independent $\Delta^g_lC_p$ value. This mix-and-match approach has the advantage of including the expected alkyl chain dependence of $\Delta^g_lC_p$ for certain ILs [111]; the clear disadvantage is the glaring inconsistency, as $\Delta^g_lC_p$ has not been determined by any method for many ILs for which $\Delta_{vap}H$ values have been measured. The second option is to use a constant, IL independent $\Delta^g_lC_p$ value for all ILs. This approach has the advantages of simplicity and consistency, but with the considerable disadvantage of missing the alkyl chain length dependence. In this contribution a constant, IL independent $\Delta^g_lC_p = -100\,J\,K^{-1}\,mol^{-1}$ was used, as this approach is a reasonable compromise, as it represents the approximate mid-point of $\Delta^g_lC_p$ values published to date.

In terms of selecting a common T, in almost all literature examples for ILs $T = 298\,K$ has been chosen; thus, $\Delta_{vap}H_{298}$ is obtained. Using $T = 298\,K$ allows ready comparison to many other properties of ILs, e.g. surface tension. However, $T = 450\,K$ has also been used to ensure that the T extrapolation is minimal, as $T = 450\,K$ is similar to the T at which $\Delta_{vap}H$ is measured [140]. In this contribution $T = 298\,K$ is used. As noted above, when using $T = 298\,K$ and $\Delta^g_lC_p = -100\,J\,K^{-1}\,mol^{-1}$, large differences can occur for certain ILs. However, $T = 450\,K$ was also tested; using $T = 450\,K$ gave the same correlation observed in figure 3*b* (see electronic supplementary material, figure S1).

4.4.3. Monitoring ionic liquid vaporization only

IL vaporization only must be measured to ensure reliable $\Delta_{vap}H$ data, i.e. the vaporization of liquid-phase non-ionic TD products must not be measured. Methods that can distinguish *in situ* between IL vaporization and vaporization of liquid-phase TD products are ideal. However, there are relatively few such methods available; for ILs, TPMS and TGA (using two carrier gases) are the main methods used for distinguishing IL vaporization and vaporization of liquid-phase TD products [31,64,65,77].

Methods that involve measuring the amount of vapour that condenses from the gas phase onto a solid surface (e.g. QCM and MSB), when operated under high vacuum conditions (i.e. apparatus base system pressure less than 10^{-8} mbar), can be used to detect only IL vaporization. ILs are clearly sufficiently involatile that they will condense onto a solid surface at room temperature, whatever the system pressure. Many TD products of ILs are highly volatile, e.g. for halide-ion ILs [77,90]. Therefore, it is expected that such volatile TD products will not condense under high vacuum conditions at room temperature. Consequently, using QCM and MSB under high vacuum conditions would detect only IL vaporization, as long as the TD products were relatively volatile. However, not all TD products for ILs are highly volatile, e.g. for $[C_nC_1Im][BF_4]$ ILs [141].

A number of popular methods of obtaining $\Delta_{vap}H$ for ILs involve measuring the total amount of vaporization. Almost all methods that involve measuring the mass lost from the liquid-phase measure the total amount of IL vaporization, e.g. TGA using only one carrier gas [108–116], Knudsen effusion mass loss [56] and calorimetry [142]. Also, some methods that involve measuring the amount of ionic vapour rely on there being no significant vaporization of liquid-phase non-ionic TD products, e.g. vapour phase spectroscopy [80,118]. Therefore, these methods rely on no significant vaporization of liquid-phase TD products occurring. In some studies attempts have been made to check if TD occurred by characterizing either the condensate or the remaining IL that had not vaporized. Neither of these approaches is foolproof. For the condensate, as noted above, TD products may be sufficiently volatile that they do not condense under experimental conditions; for the remaining IL sample, observing no TD products in the liquid phase does not mean there was no TD product vaporized.

For $[C_nC_1Im][NTf_2]$ ILs ($n = 2$ and 4) it has been demonstrated, using two carrier gas TGA, that $\Delta_{vap}H$ is far smaller than the activation energy of TD [31,64]. In addition, $[C_nC_1Im][NTf_2]$ ILs (along with $[N_{2,2,2,2}][NTf_2]$ and $[C_4C_1Pyrr][NTf_2]$) have been readily distilled without significant TD occurring [61–63]. These results indicate that for [cation][NTf_2] ILs, where the cation does not contain relatively reactive functional groups, only IL vaporization is significant under the experimental conditions generally used for vaporization experiments. Therefore, the assumption that many researchers make that only IL vaporization occurs for [cation][NTf_2] ILs appears to be valid, making $\Delta_{vap}H$ values measured for [cation][NTf_2] more trustworthy than for other ILs.

There is the absurd situation where the same technique, TGA with a single carrier gas, for the same families of ILs has been used to determine either $\Delta_{vap}H$ or the activation energy of TD, i.e. in different papers it is assumed that only IL vaporization or only liquid-phase non-ionic TD product vaporization was occurring. This situation has occurred for carboxylate-based ILs [143,144], $[NTf_2]^-$-based ILs [110,111,145,146] and Cl^--based ILs [147,148]. Therefore, when using TGA it would appear best to use at least two different carrier gases (to allow ionic vapour and TD products to be distinguished)

or only study ILs for which vaporization is known to be dominant, e.g. [cation][NTf_2]. Hence, for the correlations discussed in §§7 and 8, $\Delta_{vap}H$ values measured using TGA (and the transpiration method) for ILs other than [cation][NTf_2] ILs have been excluded. This exclusion of ILs such as [cation]Cl reflects the unknown composition of the vapour phase; such ILs are known to have relatively similar $\Delta_{vap}H$ and the activation energies of TD, and are known to thermally decompose, even under vacuum using Langmuir vaporization conditions [77,90]. For the correlations by Kabo *et al*. [140] of literature $\Delta_{vap}H$ values with ρ and γ, all TGA data were excluded due to uncertainty over the data analysis methods. However, in this article TGA data were selected based upon the ILs studied and concerns over competition from TD; the analysis methods used were trusted.

The $\Delta_{vap}H$ value from the group of Vaghjiani and co-workers for [C_4C_1Pyrr][NTf_2] is excluded from correlations here, as it appears to be a very large outlier [80] relative to the other three published $\Delta_{vap}H$ values for the same IL [73,112]. The microcalorimetry $\Delta_{vap}H$ values for [C_nC_1Im][NTf_2] are very large outliers [142] and were excluded for reasons explained in [129]. A contributing factor may have been the relatively high temperatures at which these measurements were carried out. The TPUV $\Delta_{vap}H$ data from Ogura *et al*. [149] was excluded due to the very large $\Delta_{vap}H$ values and the very large errors given.

The $\Delta_{vap}H$ values from Verevkin and co-workers for three protic ILs are excluded [150]. It is expected that the vapour phase for the three ILs studied will mainly comprise ionic vapour [67] and not non-ionic TD product vapour (most likely the products of proton transfer from the cation to the anion), but no evidence is presented to confirm this supposition. For protic ILs, ideally a $\Delta_{vap}H$ technique would be used that can distinguish between IL vaporization and TD product vaporization.

4.4.4. Comparing vaporization conditions: Knudsen effusion versus Langmuir

For ILs, both Knudsen effusion [56,86–89,91,119,129–133,135,151,152] and Langmuir [31,57,63,64,71–77,80,96,106–128] vaporization methods have been used to obtain $\Delta_{vap}H$. For Langmuir (i.e. non-equilibrium) vaporization, an activation barrier to vaporization due to the IL–gas surface structure could exist. Consequently, measurements under Langmuir vaporization conditions would not probe the vaporization energy required to obtain a reliable and accurate $\Delta_{vap}H$ value, i.e. vaporization kinetics would be contributing to any measurement.

Any possible effect of kinetics on vaporization energetics can be judged by comparing data for techniques that used near-equilibrium and far-from-equilibrium methods, e.g. Knudsen mass loss versus TPMS, respectively. For [C_nC_1Im][NTf_2], $\Delta_{vap}H$ values published in 2006 and 2007 from Knudsen cell mass loss [56] and from Langmuir vaporization [71] matched extremely well (note that the $\Delta^g_1C_p$ values used were very similar and thus no mismatch was caused by $\Delta^g_1C_p$). Since then, both near-equilibrium and Langmuir methods have confirmed agreement in $\Delta_{vap}H$ values for [C_nC_1Im][NTf_2] [111,129]. That the values are the same within the relatively small errors strongly suggests that there is no significant kinetic effect for Langmuir vaporization; therefore, there is no significant activation barrier for vaporization at the IL–gas surface. Good matches of $\Delta_{vap}H$ values from near-equilibrium and far-from-equilibrium methods have also been published for [C_nC_1Pyrr][NTf_2] and [C_nPy][NTf_2] ILs. For ILs with anions other than $[NTf_2]^-$ there is currently no data to judge kinetic effects on vaporization, as no Knudsen cell (i.e. near-equilibrium) measurements have been made for ILs with anions other than $[NTf_2]^-$. For example, for [C_4C_1Im][PF_6] the primary process for near-equilibrium conditions was vaporization of TD products [153], whereas the primary process for Langmuir evaporation was vaporization of intact IL [96]. This difference is due to the higher temperature required for near-equilibrium conditions (compared to Langmuir evaporation) to detect vaporization.

4.4.5. $\Delta_{vap}H$ values for approximately 115 ionic liquids

There is now a significant quantity of $\Delta_{vap}H$ data available in the literature (approx. 40 papers); there are $\Delta_{vap}H_{298}$ values published for approximately 115 ILs (see electronic supplementary material, table S3). $\Delta_{vap}H$ values published in the literature to date have mainly been produced by three groups, who are led principally by Verevkin, Santos and Jones. The Santos group have published only for [cation][NTf_2] ILs, whereas the Verevkin and Jones groups have published for [cation][NTf_2] ILs and also for a wider variety of anions, e.g. $[PF_6]^-$ and $[BF_4]^-$. Publications from groups other than these three groups have mainly focused on [cation][NTf_2] ILs. This concentration on [cation][NTf_2] ILs reflects firstly the wish for researchers new to the area to investigate ILs for which $\Delta_{vap}H$ values have already been published, secondly the relative thermal stability of [cation][NTf_2] ILs (as noted in §4.4.3, and quantified in [31,64]) and thirdly the large number of [cation][NTf_2] ILs that are liquid at room temperature.

4.4.6. Measuring $\Delta_{des}H$

Measuring ced_{C+A} requires V_m and either $\Delta_{des}H([C]^+)$ and $\Delta_{des}H([A]^-)$ (equation (4.3)) or $\Delta_{vap}H$ and $\Delta_{diss}H(CA)$ (equation (4.5)). Therefore, there are two potential experimental approaches to obtain ced_{C+A}.

Experimental values for $\Delta_{des}H([C]^+)$ and $\Delta_{des}H([A]^-)$ can be obtained [87,91]. These measurements have been carried out in the range of T approximately 490 K. To obtain $\Delta_{des}H([C]^+)$ and $\Delta_{des}H([A]^-)$ at $T = 298$ K, an extrapolation is required. Therefore, the heat capacity at constant pressure for the isolated ions in the vapour phase will be required (the heat capacity for the liquid phase can be measured, as noted in §4.4.2). At present, these values are not available, although they could be readily calculated.

$\Delta_{diss}H(CA)$ has not been measured experimentally to date. For a $[C_2C_1Im][NTf_2]$ ionic vapour neutral ion pair the energy to produce electronically excited but bound $([C_2C_1Im][NTf_2])^*$ was found to be 5.5 eV, i.e. 531 kJ mol^{-1} [85]. This value represents an upper limit for $\Delta_{diss}H(CA)$ for $[C_2C_1Im][NTf_2]$.

4.5. Obtaining the cohesive energy density from simulations and calculations

$\Delta_{vap}H$ can be obtained using simulations and calculations. Enthalpies for the ionic vapour neutral ion pair can be calculated using high-level methods. The most widely used approach to obtain the liquid-phase enthalpy per ion pair is from molecular dynamics simulations [26,154–156]; an ion pair in a continuum solvation model has also been used [157,158]. V_m can also readily be obtained from molecular dynamics simulations; hence, ced_{IP}(calc.) can be obtained from simulations and calculations for ILs.

$\Delta_{des}H$(total) (i.e. $ce_{C+A} + 2RT$) can be obtained either from a combination of experimental ($\Delta_{vap}H$, table 1) and calculated ($\Delta_{diss}H_{298}$(CA), table 2) [103] results or solely from calculations [104]. $\Delta_{diss}H(CA)$ values have been published for many ILs (e.g. [103,196,197]). A combination of simulations and calculations has been used for ILs to obtain ce_{C+A} for a limited selection of ILs ($[C_nC_1Im][BF_4]$ and $[C_nC_1Im][PF_6]$, where $n = 2, 4, 6$) [104]; ced_{C+A} were not provided in the article.

As explained in §3.3, δ_H (and therefore ced_{ML}) can be separated, using indirect methods, into non-polar, polar and hydrogen bonding contributions [15]. For ILs, at least two different methods have been used to obtain contributions to ced_{IP} (or contributions to $\Delta_{vap}H$, from which contributions to ced_{IP} can be obtained), and these methods are explained in the next two paragraphs. Methods to separate the different contributions to intermolecular interactions, and which contributions get grouped together, can vary widely between different researchers.

Electrostatic contributions are generally those from Coulomb's Law; vdW interactions are usually considered as all other intermolecular interactions (therefore, induction, dispersion and hydrogen bonding are included) [155,196]. $\Delta_{vap}H$ can be separated into electrostatic and vdW contributions [155,156]. To obtain the electrostatic and vdW contributions to ced_{IP}, the electrostatic and vdW contributions to $\Delta_{vap}H$ simply need to be divided by V_m. To obtain the electrostatic and vdW contributions to ced_{C+A}, the electrostatic and vdW contributions to $\Delta_{des}H$(total) (or $\Delta_{vap}H + \Delta_{diss}H(CA)$) need to be divided by V_m. Such information is available in the literature [155,196].

A second method to separate ced_{IP} labels contributions as polar (similar to electrostatic) and non-polar (similar to vdW) [26]. These two contributions are determined by the user defining atoms in the IL that are polar and atoms that are non-polar. Interaction energies for these atoms are then summed to obtain the polar and non-polar contributions to ce_{IP} (when there is an interaction between a polar atom and a non-polar atom, the energy is shared equally). The polar and non-polar contributions to ced_{IP} are then obtained by dividing by the partial liquid volumes for the polar and non-polar atoms, respectively.

5. Results for $\Delta_{vap}H$, $\Delta_{des}H([C]^+)$ and $\Delta_{des}H([A]^-)$ for ionic liquids

$\Delta_{vap}H$ for ILs are much larger than $\Delta_{vap}H$ for MLs, as expected. $\Delta_{vap}H_{298}$ values for the ILs investigated to date range from approximately 130 kJ mol^{-1} for $[C_nC_1Im][NTf_2]$ ($n = 1$ to 3) to 199 kJ mol^{-1} for $[P_{6,6,6,14}][BF_4]$ (table 1 and electronic supplementary material, table S4). For molecular liquids, $\Delta_{vap}H_{298}$ ranges from 30 kJ mol^{-1} for hexane to 102 kJ mol^{-1} for triethanolamine and 105 kJ mol^{-1} for squalane; for water $\Delta_{vap}H_{298} = 44$ kJ mol^{-1} [32,33,198].

5.1. $\Delta_{vap}H$ from experiments: trends for ionic liquids

For ILs, $\Delta_{vap}H$ values increase as n is increased (either on the cation or the anion). This conclusion has been demonstrated for $[C_nC_1Im][NTf_2]$ (figure 2*b*) [56,71,108,111,129], $[C_nC_1Im][NPf_2]$ [108,118],

Table 1. $\Delta_{vap}H_{298}$, V_m (at 298 K), V_{mol} (at 298 K), γ (at 298 K), G (at 298 K) and $ced_{IP,298}$ data for ILs (for which all of this data could be found in the literature from experimental measurements). For $\Delta_{vap}H_{298}$ and $ced_{IP,298}$ a constant $\Delta^{g}_{l}C_p = -100$ J K^{-1} mol^{-1} value was used in all cases. $\Delta_{vap}H_{298}$ values were determined for each IL by taking the average (see electronic supplementary material, table S4) of all reliable individual $\Delta_{vap}H_{298}$ literature values (how these individual $\Delta_{vap}H_{298}$ values were chosen is explained in §4.4.3). All literature references used to obtain $\Delta_{vap}H_{298}$, V_m, V_{mol} (liquid density, ρ, for both V_m and V_{mol}) and γ are given. .

ionic liquid	$\Delta_{vap}H_{298}$ kJ mol^{-1}	ref. for $\Delta_{vap}H_{298}$	V_m cm^{-3} mol^{-1}	V_{mol} nm^{-3}	ref. for ρ	γ mN^{-1} m^{-1}	ref. for γ	G J cm^{-3}	$ced_{IP,298}$ J cm^{-3}
$[C_1C_1Im][NTf_2]$	132	[111,132]	241	0.400	[55]	36.3	[55]	49.3	539
$[C_2C_1Im][NTf_2]$	136	[56,57,71,86,106,108,111,117,118,129]	257	0.427	[159]	36.9	[160]	49.1	519
$[C_3C_1Im][NTf_2]$	131	[111,129]	275	0.456	[161]	34.9	[160]	45.3	469
$[C_4C_1Im][NTf_2]$	136	[56,71,88,108,111,113,118,129]	292	0.486	[55]	33.6	[160]	42.8	457
$[C_5C_1Im][NTf_2]$	138	[111,129]	309	0.513	[161]	32.9	[160]	41.1	439
$[C_6C_1Im][NTf_2]$	142	[56,71,108,111,129]	328	0.545	[55]	32.3	[160]	39.6	425
$[C_7C_1Im][NTf_2]$	143	[111,129]	341	0.567	[162]	32.0	[160]	38.7	412
$[C_8C_1Im][NTf_2]$	149	[56,71,108,111,129]	363	0.603	[55]	31.9	[160]	37.8	403
$[C_{10}C_1Im][NTf_2]$	152	[108,111,129]	397	0.659	[55]	32.1	[160]	36.9	378
$[C_{12}C_1Im][NTf_2]$	156	[111,129]	427	0.710	[55]	32.3	[163]	36.2	358
$[C_3C_1C_1Im][NTf_2]$	142	[86,108,152]	288	0.478	[164]	41.0	[165]	52.4	485
$[C_4C_1C_1Im][NTf_2]$	145	[121,152]	306	0.509	[166]	37.4	[167]	46.9	466
$[C_3(C_1Im)_2][NTf_2]_2$	183	[94]	476	0.791	[168]	44.7	[168]	48.3	378
$[Me(EG)_1C_1Im][NTf_2]$	130	[115]	280	0.465	[169]	35.6	[169]	45.9	455
$[Me(EG)_2C_1Im][NTf_2]$	136	[115]	320	0.531	[55]	36.5	[55]	45.1	419
$[C_2C_2Im][NTf_2]$	126	[130]	275	0.457	[170]	35.6	[163]	46.2	450
$[C_3C_3Im][NTf_2]$	131	[130]	310	0.515	[170]	32.4	[163]	40.4	416
$[C_4C_4Im][NTf_2]$	134	[130]	344	0.571	[170]	31.1	[163]	37.5	383
$[C_5C_5Im][NTf_2]$	142	[130]	379	0.629	[170]	30.1	[163]	35.1	368
$[C_6C_6Im][NTf_2]$	157	[130]	412	0.685	[170]	29.5	[163]	33.5	373
$[C_7C_7Im][NTf_2]$	150	[133]	445	0.740	[170]	29.3	[163]	32.4	332
$[C_8C_8Im][NTf_2]$	146	[133]	480	0.798	[170]	29.2	[163]	31.5	298
$[C_9C_9Im][NTf_2]$	150	[133]	515	0.855	[170]	29.5	[163]	31.1	286
$[C_{10}C_{10}Im][NTf_2]$	146	[133]	547	0.908	[170]	29.6	[163]	30.6	262
$[C_3C_2Im][NTf_2]$	132	[132]	292	0.485	[171]	33.4	[171]	42.5	445
$[C_3C_1Pyrr][NTf_2]$	147	[112]	284	0.472	[172]	32.5	[167]	41.8	510

(*Continued*.)

Table 1. (*Continued.*)

ionic liquid	$\Delta_{vap}H_{298}$ kJ mol^{-1}	ref. for $\Delta_{vap}H_{298}$	V_m cm^{-3} mol^{-1}	V_{mol} nm^{-3}	ref. for ρ	γ mN^{-1} m^{-1}	ref. for γ	G J cm^{-3}	$ced_{IP,298}$ J cm^{-3}
$[C_4C_1Pyrr][NTf_2]$	150	[73,112]	300	0.498	[172]	34.9	[167]	44.1	490
$[C_6C_1Pyrr][NTf_2]$	152	[73,112]	341	0.567	[173]	31.7	[173]	38.3	438
$[C_{10}C_1Pyrr][NTf_2]$	161	[112]	405	0.673	[173]	31.4	[173]	35.8	391
$[C_2Py][NTf_2]$	138	[124,131]	253	0.420	[174]	37.4	[174]	50.0	536
$[C_4Py][NTf_2]$	143	[118,124,131]	286	0.476	[174]	33.4	[174]	42.8	491
$[C_5Py][NTf_2]$	144	[124]	303	0.503	[174]	32.5	[174]	40.9	469
$[C_6Py][NTf_2]$	151	[73,124]	320	0.532	[174]	31.7	[174]	39.1	463
$[C_2C_1Im][NPf_2]$	136	[108,118]	308	0.512	[175]	33.9	[175]	42.4	432
$[C_4C_1Im][NPf_2]$	137	[104,114]	343	0.570	[175]	31.7	[175]	38.2	392
$[C_6C_1Im][NPf_2]$	139	[108]	378	0.627	[175]	30.3	[175]	35.4	361
$[C_8C_1Im][NPf_2]$	145	[108]	412	0.685	[55]	27.7	[55]	31.4	346
$[C_2C_1Im][BF_4]$	143	[73,123]	155	0.257	[175]	54.4	[175]	85.5	905
$[C_4C_1Im][BF_4]$	154	[75]	188	0.313	[175]	46.9	[175]	69.1	806
$[C_8C_1Im][BF_4]$	163	[71]	257	0.427	[55]	30.8	[55]	40.9	626
$[P_{6,6,6,14}][BF_4]$	199	[75]	605	1.005	[176]	28.3	[176]	28.2	325
$[C_4Py][BF_4]$	161	[73,127]	184	0.305	[177]	46.6	[177]	69.2	860
$[^3C_1{}^1C_4Py][BF_4]$	153	[127]	200	0.333	[178]	44.8	[178]	64.7	752
$[^4C_1{}^1C_4Py][BF_4]$	152	[127]	200	0.333	[178]	45.5	[178]	65.6	746
$[C_2C_1Im][C_2SO_4]$	155	[57,123]	191	0.317	[179]	47.0	[179]	68.9	800
$[C_2C_1Im][C_8SO_4]$	172	[123]	292	0.485	[180]	31.0	[180]	39.5	580
$[C_4C_1Im][C_8SO_4]$	182	[75]	328	0.544	[181]	26.7	[181]	32.7	548
$[C_2C_1Im][TfO]$	138	[123]	188	0.312	[182]	41.3	[183]	60.9	721
$[C_8C_1Im][TfO]$	152	[71]	302	0.501	[55]	28.5	[55]	35.9	495
$[C_4C_1Im][PF_6]$	150	[96]	207	0.345	[173]	44.0	[184]	62.8	710
$[C_6C_1Im][PF_6]$	153	[96]	241	0.401	[185]	38.2	[184]	51.8	624
$[C_8C_1Im][PF_6]$	164	[71,96]	276	0.458	[55]	32.5	[55]	42.2	585
$[C_2C_1Im][SCN]$	153	[73,123]	152	0.252	[186]	57.8	[186]	91.5	993
$[C_8C_1Im][N(CN)_2]$	163	[73]	256	0.426	[187]	36.9	[188]	49.0	627

(*Continued.*)

Table 1. (*Continued.*)

ionic liquid	$\Delta_{vap}H_{298}$ kJ mol^{-1}	ref. for $\Delta_{vap}H_{298}$	V_m cm^{-3} mol^{-1}	V_{mol} nm^{-3}	ref. for ρ	γ mN^{-1} m^{-1}	ref. for γ	G J cm^{-3}	$ced_{IP,298}$ J cm^{-3}
$[C_4C_1Pyrr][N(CN)_2]$	162	[72]	198	0.329	[189]	56.4	[189]	81.7	806
$[C_2C_1Im][C(CN)_3]$	139	[122]	186	0.308	[190]	50.4	[191]	74.6	733
$[C_4C_1Im][C(CN)_3]$	143	[122]	218	0.363	[190]	49.2	[191]	69.0	643
$[C_2C_1Im][B(CN)_4]$	136	[123]	217	0.361	[192]	48.7	[191]	68.4	613
$[C_4C_1Im][FeCl_4]$	171	[73]	247	0.410	[193]	46.0	[193]	62.0	684
$[C_2C_1Im][FAP]$	126	[123]	342	0.568	[194]	32.5	[194]	39.2	361
$[C_6C_1Im][FAP]$	144	[75]	395	0.656	[194]	31.6	[194]	36.4	359
$[C_4C_1Pyrr][FAP]$	153	[73]	370	0.614	[195]	38.0	[165]	44.7	408
$[C_8C_1Im]Cl$	167	[77]	229	0.380	[55]	30.9	[55]	42.7	718
$[C_8C_1Im]I$	167	[77]	247	0.410	[55]	32.7	[55]	44.0	667

Table 2. $\Delta_{vap}H_{298}$ (constant $\Delta^{g}_{l}C_{p}$) and $ced_{IP,298}$ (constant $\Delta^{g}_{l}C_{p}$) are taken from table 1. $\Delta_{diss}H_{490}$(CA) (exp.) = $\Delta_{des}H_{490}$(total) − $\Delta_{vap}H_{490}$. $\Delta_{diss}H_{298}$(CA) (calc.) are taken from Preiss *et al.* [103]. ced_{C+A}(exp. + calc.) have been rounded to three significant figures.

ionic liquid	$\Delta_{vap}H_{298}$(exp.) kJ mol^{-1}	$ced_{IP,298}$(exp.) J cm^{-3}	$\Delta_{diss}H_{298}$(CA) (calc.) kJ mol^{-1}	$\Delta_{des}H_{298}$ (total) (calc.) kJ mol^{-1}	$ced_{C+A,298}$ (exp. + calc.) J cm^{-3}
$[C_2C_1Im][NTf_2]$	136	519	344	480	1850
$[C_4C_1Im][NTf_2]$	136	457	351	487	1650
$[C_2C_1Im][BF_4]$	143	905	372	515	3290
$[C_4C_1Im][BF_4]$	154	806	372	526	2770
$[C_4C_1Im][PF_6]$	150	710	353	503	2400
$[C_2C_1Im][C_2SO_4]$	155	800	385	540	2800
$[C_2C_1Im][SCN]$	153	993	371	524	3420
$[C_2C_1Im][C(CN)_3]$	139	733	340	479	2550

$[C_nC_1Pyrr][NTf_2]$ [73,112], $[C_nPy][NTf_2]$ [124], $[C_nC_mPy][NTf_2]$ [134], $[C_nC_1Im][PF_6]$ [96], and $[C_2C_1Im][C_nSO_4]$ [57,123]. A broad conclusion for $\Delta_{vap}H$ values is that $[NTf_2]^-$-based ILs exhibit lower $\Delta_{vap}H$ values than for ILs with anions such as $[BF_4]^-$ or $[N(CN)_2]^-$ (when the cation is the same, table 1 and electronic supplementary material, table S4). For ILs with the same anion and different cation cores, there is relatively limited data available. A broad conclusion is that, where n is the same, $[C_nC_1Im][NTf_2]$ gave lower $\Delta_{vap}H_{298}$ values than $[C_nC_1Pyrr][NTf_2]$ and $[C_nPy][NTf_2]$ (where $n = 4$ or $n = 6$) [56,71,73,108,111,112,124,129].

5.2. $\Delta_{vap}H$ from simulations and calculations

There is a vast amount of $\Delta_{vap}H$(calc.) data available in the literature, far too much to give a complete summary here. Therefore, the focus here will be on key examples. The most widely used force field for ILs is the CL&P force field [199]. The aim of the developers of this force field was to provide a model that could describe a large range of ILs; hence, only liquid-phase densities and structural data were used for parametrization [199]. $\Delta_{vap}H_{298}$(calc.) using the CL&P force field are in the range of 150 to 250 kJ mol^{-1} [23,156,199]. These $\Delta_{vap}H$(calc.) are larger than $\Delta_{vap}H$(exp.), which are in the range of 130 to 180 kJ mol^{-1} for these ILs. This finding is not surprising, given the relatively low levels of parametrization used to produce the CL&P force field. However, the trend of $\Delta_{vap}H$ values increasing as n increases is found, and $[C_4C_1Im][NTf_2]$ giving a small $\Delta_{vap}H_{298}$(calc.) relative to other $[C_4C_1Im][A]$ ILs, suggests that correct trends in intermolecular interactions are captured. Köddermann *et al.* [154,155] parametrized a force field against experimental data for $[C_2C_1Im][NTf_2]$, including structural, dynamic and thermodynamic data (liquid-phase density, self-diffusion coefficients of cations and anions and NMR rotational correlation times for cations). $\Delta_{vap}H_{298}$(calc.) for $[C_nC_1Im][NTf_2]$ ($n = 2$, 4, 6, 8) using this force field matched very well to $\Delta_{vap}H_{298}$(exp.) [56,71,154], demonstrating that force fields can be produced for ILs that do an excellent job of capturing the intermolecular interactions. Schröder and Coutinho used the continuum solvation model COSMO–RS for a structurally diverse set of ILs to obtain $\Delta_{vap}H_{298}$(calc.) [158]. $\Delta_{vap}H_{298}$(calc.) matched very well to $\Delta_{vap}H_{298}$(exp.) (±10 kJ mol^{-1}), demonstrating that the continuum solvation model captured the bulk liquid very well.

5.3. $\Delta_{des}H([C]^+)$, $\Delta_{des}H([A]^-)$ and $\Delta_{diss}H$(CA) from experiments, simulations and calculations

$\Delta_{des}H([C]^+)$ and $\Delta_{des}H([A]^-)$ have been experimentally measured for $[C_2C_1Im][NTf_2]$ only. Therefore, ced_{C+A} can only be obtained from experimental values for $[C_2C_1Im][NTf_2]$. $\Delta_{des}H_{490}([C]^+) = 206$ kJ mol^{-1} and $\Delta_{des}H_{490}([A]^-) = 207$ kJ mol^{-1} at $T \sim 490$ K. Therefore, $\Delta_{des}H_{490}([C]^+) + \Delta_{des}H_{490}([A]^-) = \Delta_{des}H_{490}$(total) = 413 kJ mol^{-1}. Using $\Delta_{des}H_{490}$(total) (exp.) = 413 kJ mol^{-1} and $\Delta_{vap}H_{490}$(exp.) = 117 kJ mol^{-1} (constant $\Delta^{g}_{l}C_{p}$) an experimentally derived value of $\Delta_{diss}H_{490}$(CA) (exp.) = 296 kJ mol^{-1} can be obtained for the first time.

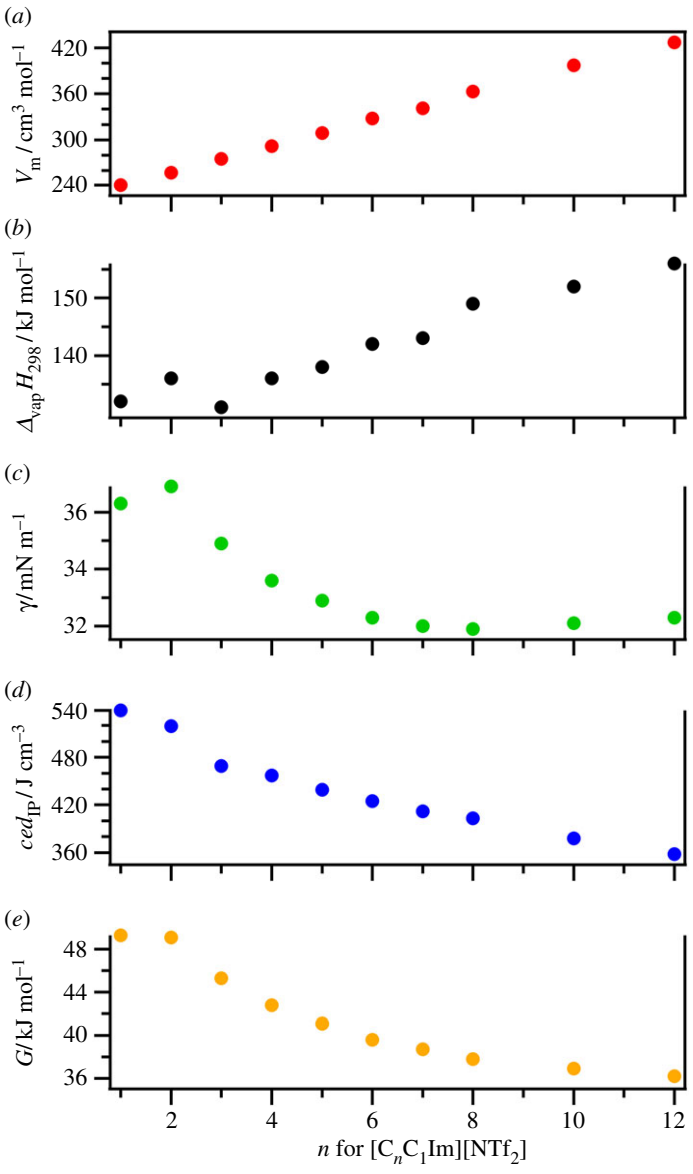

Figure 2. Variation of properties with respect to n for $[C_nC_1Im][NTf_2]$: (*a*) molar volume, V_m, (*b*) enthalpy of vaporization at 298 K, $\Delta_{vap}H_{298}$, (*c*) surface tension, γ, (*d*) cohesive energy density with an ion pair as the molecular unit, ced_{IP} and (*e*) Gordon parameter, *G*. The data used and references are given in table 1. The $\Delta_{vap}H_{298}$ values (and, therefore, the ced_{IP} values) were obtained using a constant $\Delta^g{}_lC_p = -100\ J\ K^{-1}\ mol^{-1}$; it has been discussed elsewhere how using such an approach can lead to non-linearity in $\Delta_{vap}H_{298}$ values for $[C_nC_1Im][NTf_2]$ at small n, but when variable $\Delta^g{}_lC_p$ values are used the relationship is closer to linear with respect to n [111].

Table 3. $\Delta_{vap}H_{490}$ was extrapolated using constant $\Delta^g{}_lC_p = -100\ J\ K^{-1}\ mol^{-1}$. $\Delta_{des}H_{490}([C]^+)$ and $\Delta_{des}H_{490}([A]^-)$ are taken from Dunaev *et al.* [91]. $\Delta_{diss}H_{490}(CA)\ (exp.) = \Delta_{des}H_{490}(total) - \Delta_{vap}H_{490}$. $ced_{C+A,490}$(exp.) has been rounded to three significant figures.

ionic liquid	$\Delta_{vap}H_{490}$ (exp.) kJ mol^{-1}	$\Delta_{des}H_{490}([C]^+)$ (exp.) kJ mol^{-1}	$\Delta_{des}H_{490}([A]^-)$ (exp.) kJ mol^{-1}	$\Delta_{des}H_{490}$(total) (exp.) kJ mol^{-1}	$\Delta_{diss}H_{490}$(CA) (exp.) kJ mol^{-1}	$ced_{C+A,490}$ (exp.) J cm^{-3}
$[C_2C_1Im][NTf_2]$	117	207	206	413	296	1580

For $[C_2C_1Im][NTf_2]$ $\Delta_{des}H_{490}$(total) (exp.) = 413 kJ mol^{-1} (table 3) is approximately 3½ times larger than $\Delta_{vap}H_{490}$(exp.) = 117 kJ mol^{-1} (constant $\Delta^g{}_lC_p = -100\ J\ K^{-1}\ mol^{-1}$). It takes 3½ times more energy to vaporize two isolated ions than to vaporize a neutral ion pair.

Calculated $\Delta_{diss}H_{298}$(CA) for [C_nC_1Im][A] ILs gives 340 to 430 kJ mol^{-1} at 298 K (table 2) [103]. $\Delta_{diss}H$(CA) varies very little with increasing n for the high-level calculations in [103,196], whereas for the lower-level calculations in [104] $\Delta_{diss}H$(CA) decreases with increasing n (which is a very surprising finding, given one would expect both the electrostatic and vdW interactions for a neutral ion pair to be relatively unaffected by alkyl chain length). A combination of these $\Delta_{diss}H_{298}$(CA) (calc.) values from [103] and $\Delta_{vap}H_{298}$(exp.) gave 480 kJ mol^{-1} < $\Delta_{des}H_{298}$(total) (calc.) < 540 kJ mol^{-1} (table 2).

5.4. Separating $\Delta_{vap}H$, $\Delta_{diss}H$(CA), $\Delta_{des}H([C]^+)$ and $\Delta_{des}H([A]^-)$ into electrostatic and vdW contributions

The electrostatic and vdW contributions to $\Delta_{vap}H$ obtained from molecular dynamics simulations of the liquid phase vary greatly for different ILs (and often give overestimates of the experimental $\Delta_{vap}H$ values, §5.2). The electrostatic contributions range from 60 to 200 kJ mol^{-1}, depending on the IL; the vdW contributions range from 70 to 210 kJ mol^{-1} [156]. For example, for [C_8C_1Im][NTf_2] the electrostatic and vdW contributions to $\Delta_{vap}H$ are 73 and 114 kJ mol^{-1} respectively; in contrast, for [C_4C_1Im][BF_4] the electrostatic and vdW contributions to $\Delta_{vap}H$ are 117 and 64 kJ mol^{-1}, respectively [156].

Using molecular dynamics simulations for [C_nC_1Im][NTf_2] it has been found that as n increases the electrostatic contribution stays approximately constant while the vdW contribution increases significantly [155,156]; the same has been found for [C_nC_1Im][NO_3] and [C_nC_1Im][PF_6] [26,156]. Therefore, the increase in $\Delta_{vap}H$ with increasing n is due to extra vdW contributions. For the IL [$P_{6,6,6,14}$][NTf_2], which contains 28 CH_2 groups and 4 CH_3 groups, the electrostatic and vdW contributions to $\Delta_{vap}H$ are 67 and 200 kJ mol^{-1}, respectively, demonstrating that vdW contributions can dominate for certain ILs [156].

For [C_4C_1Im][A] ILs the vdW contributions are all in the range of 60 to 100 kJ mol^{-1}, whereas the electrostatic contributions have a far larger range, from 80 to 210 kJ mol^{-1}. [C_4C_1Im][NTf_2] has a far smaller electrostatic contribution than [C_4C_1Im][BF_4]. These findings demonstrate that [C_4C_1Im][BF_4] has a larger $\Delta_{vap}H$ than [C_4C_1Im][NTf_2] due to stronger electrostatic contributions.

Electrostatic intermolecular interaction contributions dominate $\Delta_{diss}H$(CA), with vdW contributions near zero, for the ILs studied ([C_nC_1Im][A] and [C_nC_1Pyrr][A] with a wide range of anions) [155,196]. For example, for [C_2C_1Im][NTf_2] the electrostatic contribution to $\Delta_{diss}H$(CA) is actually larger than $\Delta_{diss}H$(CA) itself, i.e. the vdW interactions are stronger in the isolated $[C]^+$ and isolated $[A]^-$ than in the CA neutral ion pair [196]. Given that $\Delta_{diss}H$(CA) are always significantly larger than $\Delta_{vap}H$, this finding shows that electrostatic contributions dominate $\Delta_{des}H$.

6. Cohesive energy densities: results

As noted in §4.4.5, there are many $\Delta_{vap}H$ values available in the literature for ILs. Unsurprisingly, some of these $\Delta_{vap}H$ values have been used to obtain ced_{IP}, e.g. in [200–203]. A key difference is that in this article the $\Delta_{vap}H$ data used is rigorously selected; only $\Delta_{vap}H$ values obtained directly from heating experiments are included, and where doubts exist over the $\Delta_{vap}H$ values they are not included (as outlined in §4.4.3).

6.1. Trends in ced_{IP} for ionic liquids

$ced_{IP,298}$ values range from 262 J cm^{-3} for [$C_{10}C_{10}$Im][NTf_2] to 9932 J cm^{-3} for [C_2C_1Im][SCN] (table 1). The range for $\Delta_{vap}H_{298}$ is approximately 130 kJ mol^{-1} to approximately 200 kJ mol^{-1}. The range for V_m is approximately 150 cm^3 mol^{-1} to approximately 600 cm^3 mol^{-1}. The range for $ced_{IP,298}$ is clearly larger than for $\Delta_{vap}H_{298}$, caused by the larger range for V_m over $\Delta_{vap}H_{298}$ (table 1). A plot of $ced_{IP,298}$ against V_m^{-1} (figure 3*a*) shows a very good linear correlation ($R^2 = 0.92$). Marcus recently found a similar correlation between ced_{IP} (using $\Delta_{vap}H$ both from experimental and indirect measurements) and the ionic volume (which is proportional to V_m) [202]. This finding demonstrates conclusively that the $\Delta_{vap}H_{298}$ values are not the key factor in determining ced_{IP} for ILs; the key factor is V_m, i.e. IL size. Large ILs have small ced_{IP}, and small ILs have large ced_{IP}; size matters. ced_{IP} can now be predicted with good reliability from calculations alone with no experimental input, as you just need to know V_m (or V_{mol}), and V_m can be predicted without IL synthesis [195,204].

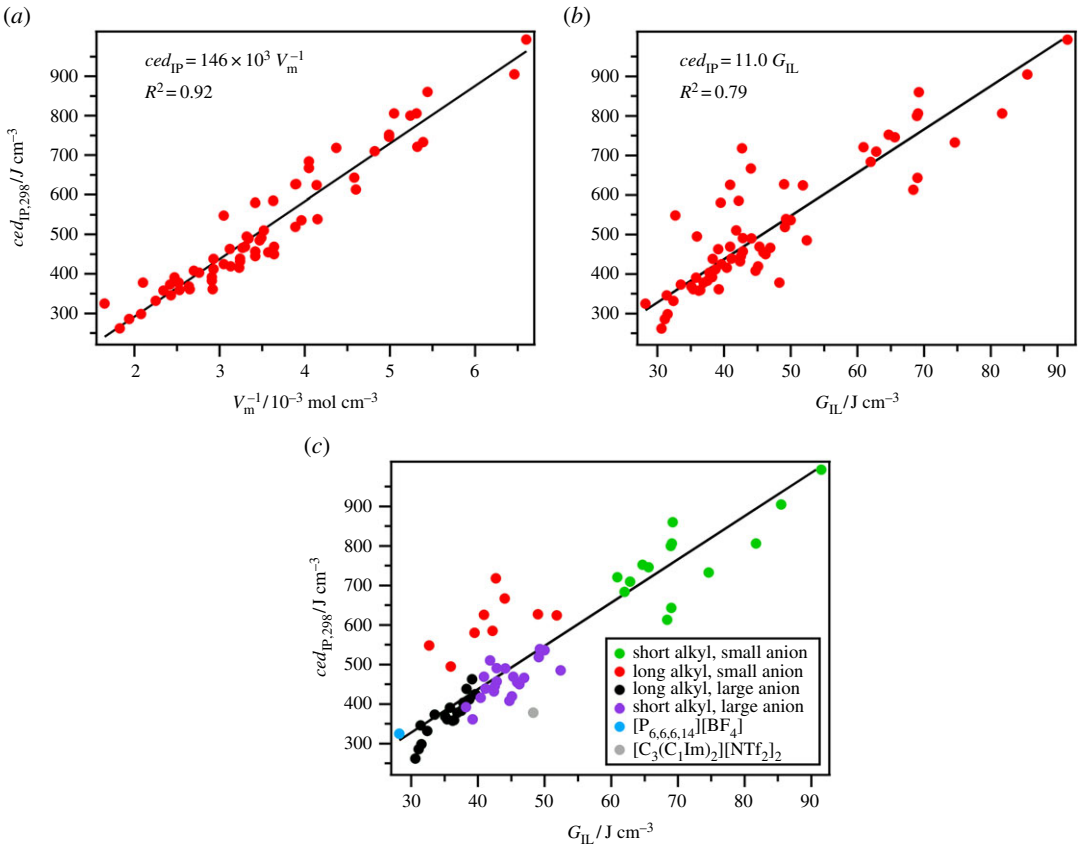

Figure 3. $ced_{IP,298}$ for ILs (extrapolated to $T = 298$ K using constant $\Delta^g_l C_p = -100$ J K^{-1} mol^{-1}) versus: (*a*) V_m^{-1}, (*b*) G_{IL}, (*c*) G_{IL}. The same data are plotted in (*b*) and (*c*); in (*c*) different IL families are plotted as the same colour data points. Details on the families are given in §7.1; $[P_{6,6,6,14}][BF_4]$ and the dicationic IL $[C_3(C_1Im)_2][NTf_2]_2$ do not fit into any of the four categories used here.

6.2. ced_{C+A} for ionic liquids

Despite $\Delta_{des}H([C]^+)$ and $\Delta_{des}H([A]^-)$ being experimentally measured for an IL, ced_{C+A} has not been obtained from the experimental data to date, as far as I am aware. For $[C_2C_1Im][NTf_2]$ experimentally derived $ced_{C+A,490} = 1580$ J cm^{-3} (rounded to three significant figures) at approximately 490 K.

$ced_{C+A,298}$ obtained from a combination of experimental ($\Delta_{vap}H_{298}$, table 1) and calculated ($\Delta_{diss}H_{298}$(CA)) results gives approximately 1600 J cm^{-3} < $ced_{C+A,298}$ < approximately 3400 J cm^{-3}. $ced_{C+A,298}$ obtained solely from calculations for $[C_nC_1Im][BF_4]$ and $[C_nC_1Im][PF_6]$ gave approximately 2000 J cm^{-3} to approximately 3200 J cm^{-3} [104].

$ced_{C+A,298}$ obtained from a combination of experimental ($\Delta_{vap}H_{298}$, table 1) and calculated ($\Delta_{diss}H_{298}$(CA)) [103] results gives approximately 1850 J cm^{-3} for $[C_2C_1Im][NTf_2]$. Given the potential for errors from both experiments (the signals to measure $\Delta_{des}H([C]^+)$ and $\Delta_{des}H([A]^-)$ in particular are very small and this measurement has only been made for one IL to date) and calculations (they have not been validated against experimental data) the match between the experimentally derived $ced_{C+A,490} = 1580$ J cm^{-3} and the value above $ced_{C+A,298} = 1850$ J cm^{-3} is good (and the T values are also different). This match gives confidence that the $ced_{C+A,298}$ values derived from a combination of experimental and calculated data give a reasonable measure of the IL total intermolecular interactions; certainly comparisons between two $ced_{C+A,298}$ values can be trusted when the difference between the two $ced_{C+A,298}$ values is large.

6.3. Separating *ced* into electrostatic and vdW contributions

There is currently little data in the literature from MD simulations for electrostatic and vdW contributions to ced_{IP}. Data needed to obtain electrostatic and vdW contributions to ced_{IP} is available [155,156], but the simple calculations have not been carried out; such data are presented in table 4. As explained in §5.2, the $\Delta_{vap}H_{298}$(calc) values in [156], and, therefore, ced_{IP}, are overestimates of the $\Delta_{vap}H_{298}$(exp.) values; it

Table 4. Separating *ced* into electrostatic and vdW contributions using a combination of simulations and calculations, along with experimental molar volume, V_m. The references given are for the simulation/calculation literature.

ionic liquid	$\Delta_{vap}U$ (vdW) kJ mol^{-1}	$\Delta_{vap}U$ (elec) kJ mol^{-1}	V_m (exp.) cm^3 mol^{-1}	ced_{IP} (exp.) J cm^{-3}	ced_{IP} (vdW) J cm^{-3}	ced_{IP} (elec) J cm^{-3}	$\delta_{H,IP}$ J cm^{-3}	$\delta_{H,IP}$ (vdW) J cm^{-3}	$\delta_{H,IP}$ (elec) J cm^{-3}	ref.
$[C_2C_1Im][NTf_2]$	42	82	258	481	162	318	21.9	12.7	17.8	[155]
$[C_4C_1Im][NTf_2]$	50	78	292	438	171	268	20.9	13.1	16.4	[155]
$[C_6C_1Im][NTf_2]$	60	78	328	421	182	237	20.5	13.5	15.4	[155]
$[C_8C_1Im][NTf_2]$	71	79	363	413	195	217	20.3	14.0	14.7	[155]
$[C_2C_1Im][NTf_2]$	89	81	258	659	345	314	25.7	18.6	17.7	[156]
$[C_4C_1Im][NTf_2]$	99	79	292	610	339	270	24.7	18.4	16.4	[156]
$[C_6C_1Im][NTf_2]$	108	76	328	561	329	232	23.7	18.1	15.2	[156]
$[C_8C_1Im][NTf_2]$	114	73	363	515	314	201	22.7	17.7	14.2	[156]
$[P_{6,6,6,14}][NTf_2]$	200	67	728	367	275	92	19.2	16.6	9.6	[156]
$[C_4C_1Im][PF_6]$	68	116	207	889	329	560	29.8	18.1	23.7	[156]
$[C_4C_1Im][BF_4]$	64	117	188	963	340	622	31.0	18.4	24.9	[156]

is expected that the vdW contributions are too large [156]. The electrostatic contributions to $ced_{IP,298}$ are between 90 and 620 J cm^{-3}, whereas the vdW contributions to $ced_{IP,298}$ are between 160 and 350 J cm^{-3}.

For $[C_nC_1Im][NO_3]$ ($n = 2, 4, 6, 8$) the polar contributions to $ced_{IP,298}$ are between 1300 and 1400 J cm^{-3} for all four ILs, whereas the non-polar contribution to $ced_{IP,298}$ are between 290 and 400 J cm^{-3} for all four ILs [26]. These values are not comparable to the values given in the previous paragraph, as their origins are very different (see §4.5).

Using data from [155] and [196] for $[C_2C_1Im][NTf_2]$, $\Delta_{des}H_{298}(elec) = 82 + 358 = 440$ kJ mol^{-1} and $\Delta_{des}H_{298}(vdW) = 42 - 16 = 26$ kJ mol^{-1}. Therefore, the electrostatic contribution to $ced_{C+A,298}$ for $[C_2C_1Im][NTf_2]$ is 1710 J cm^{-3}, whereas the vdW contribution to $ced_{C+A,298}$ is 100 J cm^{-3}. The electrostatic contribution dominates the total intermolecular interaction for $[C_2C_1Im][NTf_2]$. Such dominance is expected to hold for other ILs; compared to $[C_2C_1Im][NTf_2]$, the vdW contribution is expected to be even less important for $[C_2C_1Im][SCN]$, but more important for $[C_8C_1Im][NTf_2]$.

7. Can cohesive energy densities be used to understand other properties?

A key question to answer is: are either of the two measures of IL intermolecular interactions, ced_{IP} and ced_{C+A}, useful for understanding IL liquid-phase properties? The only way to answer that question is through obtaining data and developing trends using ced_{IP} and ced_{C+A}. At this stage only ced_{IP} can be used to understand other properties; there are insufficient experimental ced_{C+A} values to make meaningful comparisons and develop trends.

7.1. Gordon parameter, *G*

A range of methods have been used to measure γ for ILs [205]. There is a large variation in γ values for the same IL across different publications [205]. This occurrence is most likely due to impurities present in the sample. Many IL γ values are measured under conditions where water and other volatile impurities can contaminate the sample; in addition, grease-type impurities have been identified at IL–gas surfaces [206]. These contaminants are likely to affect γ.

ILs have γ values in the range of 26 to 60 mN m^{-1} [181,205,207,208]. Molecular liquids have γ values in the range of 18 to 72 mN m^{-1} [209–211]. Therefore, ILs and molecular liquids have γ values of the same magnitude (unlike $\Delta_{vap}H_{298}$). For ILs, γ values decrease as n is increased [205]. It is more difficult to draw conclusions on the effect of the anion on IL γ values, due to both anion complexity and variations in γ values across different publications. However, a broad conclusion is that $[NTf_2]^-$-based ILs exhibit lower γ values than for ILs with anions such as $[BF_4]^-$ or $[N(CN)_2]^-$ (for the same cation) [205].

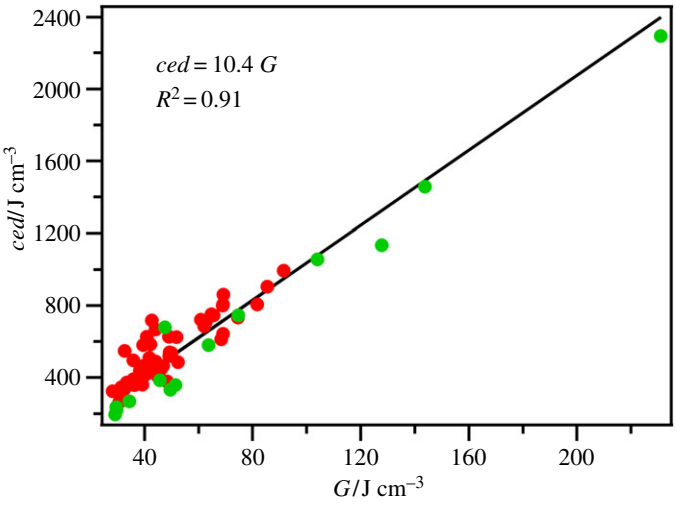

Figure 4. *ced* (including both ced_{ML} and ced_{IP}) versus *G* (including *G* for ILs and *G* for a selection of molecular liquids).

γ and $\Delta_{vap}H$ are not linearly correlated. This observation is most readily highlighted by considering the effect of increasing the alkyl chain length, *n*; $\Delta_{vap}H$ increased and surface tension decreased (e.g. for $[C_nC_1Im][NTf_2]$, figure 2*b*,*c*). Most importantly, this observation clearly demonstrates that γ and $\Delta_{vap}H$ should not be used for quantfying the strength of intermolecular interactions of ILs; comparisons need to be made for values in the same units.

G values range from 28.2 J cm^{-3} for $[P_{6,6,6,14}][BF_4]$ to 91.5 J cm^{-3} for $[C_2C_1Im][SCN]$ (for those ILs for which experimental $\Delta_{vap}H$ values are also available, table 1). *G* for molecular liquids range from 29 J cm^{-3} for squalane, 48 J cm^{-3} for ethanol, 128 J cm^{-3} for glycerol and 231 J cm^{-3} for water (electronic supplementary material, table S5).

There is a good linear correlation between ced_{IP} and *G* for ILs (figure 3*b*). Marcus recently found a similar correlation between ced_{IP} (using $\Delta_{vap}H$ both from experimental and indirect measurements) and *G* [212]. This observation strongly suggests that ced_{IP} and *G* both capture the same intermolecular interactions for ILs. *G* shows a good linear correlation with the inverse of size, V_m^{-1}, i.e. a small IL has a large *G* value (electronic supplementary material, figure S2). This is as expected, given the correlations given previously, and reiterates that the strength of intermolecular interactions in ILs can be obtained, to a good degree of accuracy, from their size.

There is a good linear correlation between *ced* and *G* when both molecular and ILs are considered (figure 4). This relationship strongly suggests that there is an underlying relationship between *ced* and *G* that is not dominated by the ionic nature of ILs.

Although a major aim of this article is to find correlations that hold across all ILs, it is important to compare ced_{IP} and G_{IL} for select IL families/categories. Categorizing the ILs in figure 3 into different families is potentially arbitrary. ILs with a large anion [75,195] ($[NTf_2]^-$, $[NPf_2]^-$ and $[FAP]^-$) are grouped together here. It must be noted that $[C_4SO_4]^-$ and $[C_8SO_4]^-$ are relatively large, but this is caused by the large alkyl chain, and hence these anions are classified here as small (the reasons for this classification will become clear shortly). ILs with small anions are categorized here as all those that do not contain $[NTf_2]^-$, $[NPf_2]^-$ or $[FAP]^-$.

For ILs with a large anion and any length alkyl chain both ced_{IP} and G_{IL} were relatively small (figure 3*c*), as all data points are located in the bottom left of figure 3*c*. In addition, all of these ILs with large anions match relatively well to the line of best fit for all ILs, first presented in figure 3*b*. Within that family, ILs with long alkyl chains (defined here as having at least one alkyl chain of length C_6H_{13}, i.e. $[C_6C_1Im][NTf_2]$, although ILs with two intermediate alkyl chains were also included in this category, i.e. $[C_4C_4Im][NTf_2]$) are coloured black (figure 3*c*), and ILs with short alkyl chains are coloured purple (figure 3*c*). Clearly, ILs with long alkyl chains gave smaller ced_{IP} and G_{IL} than those with long short alkyl chains.

ILs with small anions and short alkyl chains (plotted as green points on figure 3*c*) gave the largest ced_{IP} and G_{IL}. Therefore, to obtain an IL with the combination of both a large ced_{IP} and a large G_{IL} a short alkyl chain and a small anion is required. ILs with small anions and long alkyl chains (plotted as red points on figure 3*c*) gave relatively large ced_{IP} but smaller than expected G_{IL}, based upon their ced_{IP}. While conclusions based on individual data points should be treated with caution,

Table 5. Aprotic ILs which are known to support amphiphile self-assembly [40] and for which ced_{IP} and G have also been measured.

ionic liquid	$ced_{IP,298}$ / J cm^{-3}	G_{IL} /J cm^{-3}
$[C_4C_1Im][NTf_2]$	457	42.8
$[C_2C_1Im][NTf_2]$	519	49.1
$[C_4C_1Im][PF_6]$	710	62.8
$[C_2C_1Im][C_2SO_4]$	800	68.9
$[C_4C_1Im][BF_4]$	806	69.1
$[C_4C_1Pyrr][N(CN)_2]$	806	81.7

the presence of a cluster of red data points (figure 3*c*) suggests that the relationship for ILs with small anions and long alkyl chains is different to other ILs reported here. One possible explanation for this observation for ILs with small anions and long alkyl chains is the influence of the IL–gas surface structure on G_{IL}. There is a large amount of literature showing that ILs tend to orient with their longer alkyl chains, on average, at the outer IL–gas surface, with the rest of the IL, on average, located just below the outer IL–gas surface [213,214]. Intermolecular interactions for alkyl chains are weaker than those for the other parts of the ILs (e.g. ion–ion electrostatic intermolecular interactions). Therefore, having more alkyl chains located near the outer IL–gas surface than expected based on the stoichiometry will lead to lower G_{IL} but will have no effect on ced_{IP}. At this stage, there is insufficient evidence to draw this conclusion with high confidence, but there is a growing amount of evidence to support it.

7.2. Ionic liquids as solvents for self-assembly

In 2013 a summary was presented of aprotic ILs that support amphiphile self-assembly; at least 11 aprotic ILs were found, in addition to at least 37 protic ILs [40]. ILs that promote self-assembly for which ced_{IP} and G have also been measured are listed in table 5. Clearly, the rule [13,14] given by Evans of self-assembly only occurring in solvents with $G > 110\,\mathrm{J\,cm^{-3}}$ does not hold. The lower limit from this data would appear to be $G_{IL} > 42.8\,\mathrm{J\,cm^{-3}}$ and $ced_{IP} > 457\,\mathrm{J\,cm^{-3}}$. This would suggest that any IL with G_{IL} and ced_{IP} greater than these values would be able to support self-assembly. ILs that meet these criteria include $[C_6C_1Im][PF_6]$ and $[C_8C_1Im][N(CN)_2]$. Certain ILs meet the ced_{IP} rule but not the G rule, e.g. $[C_8C_1Im]Cl$ and $[C_4C_1Im][C_8SO_4]$. This lack of agreement between ced_{IP} and G_{IL} may well be due to the influence of the IL–gas surface structure, as outlined in §7.1. Therefore, ced_{IP} would appear not to be the best guide for determining self-assembly in ILs; G_{IL} is a much better guide for determining whether an IL can support self-assembly.

7.3. Solubility

$\delta_{H,indirect}$ for ILs have been obtained from activity coefficients at infinite dilution, giving $19\,\mathrm{J^{1/2}\,cm^{-3/2}} < \delta_{H,indirect} < 30\,\mathrm{J^{1/2}\,cm^{-3/2}}$ [50,200,201,215–218] and, therefore, $350\,\mathrm{J\,cm^{-3}} < ced_{indirect} < 900\,\mathrm{J\,cm^{-3}}$. At present, comparisons of ced_{IP} and $ced_{indirect}$ obtained from measurements of δ_H for ILs are difficult, as there is insufficient data to draw conclusions across a sufficiently large dataset. Marcus has compared $\delta_{H,IP}$ for ILs (obtained from ced_{IP} data) with the solubility of liquid organic solutes in ILs [203]. The ced_{IP} data (and therefore, $\delta_{H,IP}$ for ILs) were obtained from both experimental $\Delta_{vap}H$ values and $\Delta_{vap}H$ from less reliable indirect/calculation methods. However, as outlined in §6.1, there is an excellent correlation of ced_{IP} and V_m^{-1}, so less reliable $\Delta_{vap}H$ values are unlikely to have a large effect on ced_{IP} values. Therefore, the findings in this paper are expected to hold if only experimental $\Delta_{vap}H$ values were used to obtain ced_{IP}. Overall, no satisfactory correlation was found, demonstrating that the theories that underpin the use of δ_H for predicting solubilities do not hold for ILs, at least for organic solutes.

Hansen solubility parameters have been obtained for a range of ILs using indirect methods [219–222]. These values could potentially be compared to $\delta_{H,IP}$(vdW) and $\delta_{H,IP}$(elec) (obtained from ced_{IP}(vdW) and ced_{IP}(elec) respectively), examples of which are given in table 4, even though the categories are different. However, at this stage there is insufficient data both in terms of Hansen solubility parameters from indirect measurement and ced_{IP}(vdW) and ced_{IP}(elec) to make satisfactory comparisons.

7.4. Viscosity

ced values for ILs have been estimated from viscosity measurements of ILs and IL-based solutions [166,221,223–227]. These give values in the range $600\,\mathrm{J\,cm^{-3}} < ced_{\mathrm{indirect}} < 900\,\mathrm{J\,cm^{-3}}$. At present, as for data from measurements of solubility, there is an insufficiently large dataset to draw definitive conclusions on any correlations with ced_{IP}. Very recently, a linear correlation has been presented between *ce* and $E_{\mathrm{a,vis}}$ for three protic ILs [228]. $C = 5$ was found, for $ce_{\mathrm{IP}} = C \cdot E_{\mathrm{a,vis}}$. The $\Delta_{\mathrm{vap}}H$ values used to obtain this correlation were not included in correlations in this article, for reasons outlined in §4.4.3. It is assumed that, at temperatures at which the vaporization measurements were made, the unit of viscous flow in the liquid phase was ion pairs. In such a situation, using data based on $\Delta_{\mathrm{vap}}H$ and not $\Delta_{\mathrm{des}}H$(total) makes sense.

7.5. Conclusions of ced_{IP} versus ced_{indirect}

Indirect methods of obtaining ced_{indirect} for ILs (i.e. intrinsic viscosity or solubility data) have so far proved unsuccessful in matching ced_{IP} data. There are a number of possible reasons for this finding: insufficient/poor quality data (ILs are known for containing impurities), entropy may be vital (especially for solubility), ILs are large and only need to break select intermolecular interactions for processes such as solvation or new surface formation to occur, and the importance of non-polar interactions in ILs (non-polar interactions are known to cause problems for δ_{H} [15,49]). These last reasons would suggest that an approach similar to the Hansen solubility parameter approach might prove useful, if reliable data can be obtained.

8. Insights from cohesive energy densities of ionic liquids

8.1. Ionic liquids have very large total intermolecular interactions

As explained in §2.2 and §4.3, ced_{ML} and $ced_{\mathrm{C+A}}$ (but not ced_{IP}) represent the total intermolecular interactions, i.e. the total cohesion in a unit volume. $ced_{\mathrm{ML},298}$ values range from $195\,\mathrm{J\,cm^{-3}}$ for squalane, through $385\,\mathrm{J\,cm^{-3}}$ for acetone, $679\,\mathrm{J\,cm^{-3}}$ for ethanol and finishing with $2293\,\mathrm{J\,cm^{-3}}$ for water [32]. For $[C_2C_1\mathrm{Im}][\mathrm{NTf_2}]$ experimentally derived $ced_{\mathrm{C+A}} = 1576\,\mathrm{J\,cm^{-3}}$ at approximately 490 K. Clearly, $[C_2C_1\mathrm{Im}][\mathrm{NTf_2}]$ has stronger intermolecular interactions than most molecular liquids. Furthermore, based upon computationally derived $ced_{\mathrm{C+A}}$ values, some ILs have stronger intermolecular interactions than water. However, ILs certainly have significantly weaker intermolecular interactions than classical molten salts; Marcus has estimated $ced_{\mathrm{C+A}}$ for molten salts ranging from 6241 for CsI to $64\,520\,\mathrm{J\,cm^{-3}}$ for LiF [229]. Based upon the values for both ced_{IP} and $ced_{\mathrm{C+A}}$ presented here, ILs have very strong intermolecular interactions (many larger than water). Calculations and simulations indicated that these very strong intermolecular interactions are because ILs are ionic (§6.3); overcoming the electrostatic interactions to break charge neutrality costs a great deal of enthalpy per ion pair.

8.2. Intermolecular interactions for ions in the liquid phase versus ions in the vapour phase

A very simplistic, but potentially insightful, model can be developed for $[C_2C_1\mathrm{Im}][\mathrm{NTf_2}]$, given the large amount of data available for this IL. Liquid-phase molecular dynamics simulations for $[C_2C_1\mathrm{Im}][\mathrm{NTf_2}]$ gives the number of neighbouring cations surrounding an anion as approximately seven [230]. Therefore, $\Delta_{\mathrm{des}}H_{490}(\mathrm{total}) = 413\,\mathrm{kJ\,mol^{-1}}$ can be viewed as the enthalpy to break 14 cation–anion intermolecular interactions (as seven cation–anion intermolecular interactions need to be broken for the cation and seven for the anion). Consequently, each cation–anion intermolecular interaction is approximately $30\,\mathrm{kJ\,mol^{-1}}$. $\Delta_{\mathrm{diss}}H_{490}(\mathrm{CA}) = 296\,\mathrm{kJ\,mol^{-1}}$ is the enthalpy to break one cation–anion intermolecular interaction in the vapour phase. Very clearly, the vapour phase CA intermolecular interaction is substantially stronger than the average liquid-phase CA intermolecular interaction. This stronger vapour phase intermolecular interaction is most likely because having just one cation and one anion, with no other electrostatic intermolecular interactions that might weaken this one interaction, would lead to a particularly strong single electrostatic CA intermolecular interaction.

Given the strength of the liquid-phase total intermolecular interactions for ILs, $\Delta_{\mathrm{vap}}H$ values are actually smaller than one might expect. The reason for this is that vapour phase cation–anion intermolecular interactions are very strong.

8.3. Ionic liquids are associated liquids

$r(ced_{IP})$ and $r(ced_{C+A})$ are the ratios between P_{int} and ced_{IP} and ced_{C+A}, respectively. For ILs, $0.60 < r(ced_{IP}) < 0.85$ when ced_{IP} values are used, e.g. for $[C_2C_1Im][NTf_2]$ $r(ced_{IP}) = 0.81$. Therefore, ced_{IP} is considerably larger than P_{int} for all ILs [54]. These $r(ced_{IP})$ values are similar to what are collectively termed associated/tight/stiff liquids, e.g. acetone ($r = 0.67$), *n*-hexanol ($r = 0.65$) [54]. For $[C_2C_1Im][NTf_2]$ $ced_{C+A,490} = 1580\,J\,cm^{-3}$ and $P_{int} = 392\,J\,cm^{-3}$ [54,231]; therefore, $r(ced_{C+A}) = 0.25$. This $r(ced_{C+A})$ value still leads to categorization of $[C_2C_1Im][NTf_2]$ as an associated liquid, but puts $[C_2C_1Im][NTf_2]$ in the region of methanol ($r = 0.33$) and formamide ($r = 0.36$); $r = 0.07$ for water, $r = 0.24 \pm 0.02$ for liquid metals [232] and $r < 0.10$ for molten salts [232]. Overall, ILs would be classified as having stronger attractive intermolecular interactions than fluorocarbons, but weaker attractive intermolecular interactions than liquid metals, molten salts and water.

8.4. The importance of charge neutrality

ced_{C+A} values are much larger than ced_{IP} values (tables 2 and 3). V_m used to calculate both ced_{IP} and ced_{C+A} are obviously the same, so the very large difference is caused by the intermolecular interactions that are broken for vaporization of neutral ion pairs and isolated ions, respectively.

Values obtained from both intrinsic viscosity and solubility measurements are in the range of $350\,J\,cm^{-3} < ced_{indirect} < J\,cm^{-3}$. These values match the magnitude of the experimental values for ced_{IP} ($250\,J\,cm^{-3} < ced_{IP} < 1000\,J\,cm^{-3}$) and are very different from both the experimental value for ced_{C+A} and also the ced_{C+A} values obtained via indirect methods ($1550\,J\,cm^{-3} < ced_{C+A} < 3400\,J\,cm^{-3}$). In addition, there is the good linear correlation between *ced* and *G* for a dataset including both ILs and molecular liquids, where ced_{IP} is used for ILs. All of this evidence indicates that the intermolecular interactions that are broken for ILs when measuring ced_{IP} are similar to those broken for ILs when measuring $ced_{indirect}$.

A possible rationalization for the above observations centres on maintaining charge neutrality. When breaking intermolecular interactions to either form holes in a liquid or to form a new IL–gas surface, charge neutrality will be maintained, i.e. all ions will always have at least two close-contact neighbours [230], and no ion will be left without a counterion. In essence, in the liquid phase, charge neutrality is always maintained. For IL vaporization the ionic vapour is composed almost exclusively of neutral ion pairs; therefore, charge neutrality is also maintained, as every ion has a counterion present. Therefore, the physical processes that underpin $ced_{indirect}$, *G* and ced_{IP} all maintain charge neutrality. However, for ion desorption all intermolecular interactions are broken; therefore, the processes that underpin ced_{C+A} break charge neutrality. Therefore, it is possible that ced_{IP}—rather than ced_{C+A}—is the key value for understanding other properties that are underpinned by the strength of IL intermolecular interactions, even though ced_{IP} is not a measure of the total IL intermolecular interactions.

8.5. Why are ionic liquids involatile compared to molecular liquids?

A key question is: why are ILs so involatile compared to molecular liquids? Is it because ILs have very strong electrostatic intermolecular interactions in the liquid phase? ced_{IP} is a measure of the strength of intermolecular interactions that control IL vaporization. There are both liquid-phase and vapour-phase intermolecular interactions that contribute to $\Delta_{vap}H$ and therefore, ced_{IP} (see equation (8.1), which is simply equation (4.4) rearranged).

$$\Delta_{vap}H = \Delta_{des}H(\text{total}) - \Delta_{diss}H(\text{CA}). \tag{8.1}$$

For ILs, electrostatic intermolecular interactions dominate the total intermolecular interactions in the liquid phase, relative to the vdW intermolecular interactions (i.e. electrostatic intermolecular interactions control $\Delta_{des}H$, see §6.3). However, contributions of electrostatic intermolecular interactions are relatively large for the vapour phase of ILs (i.e. for $\Delta_{diss}H$). Consequently, the contribution of electrostatic intermolecular interactions to $\Delta_{vap}H$ for ILs is not dominant; as the liquid and vapour phase electrostatic contributions are similar in magnitude they subtract (see equation (8.1)) to give a relatively small electrostatic contribution to $\Delta_{vap}H$. Certain ILs have electrostatic contributions to $\Delta_{vap}H$ of approximately $60\,kJ\,mol^{-1}$ (see §5.4), which is significantly less than $\Delta_{vap}H$ for certain molecular liquids, e.g. $\Delta_{vap}H = 102\,kJ\,mol^{-1}$ for triethanolamine [32]. Hence, it can be concluded that electrostatic intermolecular interactions are not the dominant factor controlling the large $\Delta_{vap}H$ of ILs (relative to molecular liquids); vdW intermolecular interactions are important. These observations contradict the

theory that the low volatility of ILs is due to their ionic nature, i.e. their strong electrostatic intermolecular interactions [24–27].

Having established that vdW intermolecular interactions matter for ILs for controlling $\Delta_{vap}H$, it is important to understand what determines the contribution of these vdW intermolecular interactions. For the intermolecular interaction vdW contributions, size matters. The vdW contributions to $\Delta_{vap}H$ for many, if not all, ILs are expected to be significantly larger than $\Delta_{vap}H$ for water. $[C_8C_1Im][NTf_2]$ is far larger than water, so for $[C_8C_1Im][NTf_2]$ the vdW contribution to $\Delta_{vap}H$ is much larger than for water. The relatively large vdW contributions in ILs are not due to stronger vdW intermolecular interactions; there are simply more such vdW intermolecular interactions for ILs, as ILs are significantly larger than most molecular liquids. It is the same argument as to why certain hydrocarbons, e.g. squalene, have relatively large $\Delta_{vap}H$ but small ced_{ML} (see §2.3) [33].

Clearly, ILs are less volatile than molecular liquids. However, ILs can actually be considered more volatile than their liquid-phase intermolecular interactions alone would suggest. The large contribution from the vapour phase intermolecular interactions, determined by $\Delta_{diss}H$(CA), effectively cancels out a large amount of the liquid-phase intermolecular interactions contributing to $\Delta_{vap}H$ (see equation (8.1)).

8.6. Why are ced_{IP} and V_m^{-1} linearly correlated?

Both $\Delta_{vap}H$ and V_m feature in the ced_{IP} equation (equation (4.1)). However, there is a very good linear correlation between ced_{IP} and V_m^{-1} (figure 3*a*, and no correlation between $\Delta_{vap}H_{298}$ and V_m^{-1}), showing that V_m is a far more important variable for ced_{IP} than $\Delta_{vap}H$. The range of $\Delta_{vap}H_{298}$ values for ILs is relatively small, 130 to 200 kJ mol^{-1}, approximately 50% increase from the smallest to the largest value. The range of V_m, 150 to 600 cm^3 mol^{-1} (table 1), approximately 400% increase from the smallest to the largest value. Hence, V_m is a far more important variable in ced_{IP} than $\Delta_{vap}H_{298}$. V_m does not dominate ced_{ML}, i.e. $\Delta_{vap}H_{298}$ is an important variable for ced_{ML} (electronic supplementary material, table S5) [32]. It is important to unpack why this is the case.

The relatively small variation in $\Delta_{vap}H_{298}$ for ILs with a large variation in structures reflects that all ILs have considerable electrostatic and vdW intermolecular interaction contributions to $\Delta_{vap}H_{298}$ (§5.4), and that large changes in IL structure, and hence large changes in V_m, do not have a significant impact on these contributions. Additionally, increasing IL size can either increase or decrease $\Delta_{vap}H$. When n is increased (i.e. V_m^{-1} decreased) from $n = 2$ to $n = 8$, $\Delta_{vap}H_{298}$ increases (§5.1). When the anion size is increased (i.e. V_m^{-1} decreased) from $[BF_4]^-$ to $[NTf_2]^-$, $\Delta_{vap}H_{298}$ decreases (§5.1). So by increasing V_m, it is possible either to increase or decrease $\Delta_{vap}H_{298}$. Hence, a large change in V_m can lead to a small change in $\Delta_{vap}H_{298}$. Therefore, it is understandable why $\Delta_{vap}H_{298}$ and V_m^{-1} are not correlated, and furthermore, why V_m^{-1} dominates ced_{IP}.

9. Outlook: the challenges remaining

Knowledge of cohesive energy density, *ced*, for ILs has advanced a great deal in recent years. It is no longer acceptable to state that *ced* cannot be directly experimentally measured for ILs. Significant progress has been made on using *ced* values for ILs to test theories of intermolecular interactions developed for molecular liquids.

There are many challenges ahead for experimental measurements of *ced* for ILs; there are also challenges for calculations and simulations related to *ced*. Many of these challenges are focused around making vaporization measurements for ILs that do not contain the $[NTf_2]^-$ anion; IL vaporization using Knudsen effusion apparatus has only been successfully achieved for [cation][NTf_2] ILs to date. A summary of areas that could be explored are given in table 6.

10. Conclusion

ced_{ML} values have historically been very useful for understanding properties of molecular liquids, both as liquids and as solvents. For ILs, a general conclusion would be that many attempts at correlations between ced_{IP} and another property have proven unsuccessful to date. The lack of a correlation in itself can provide useful information about the underlying assumptions involved in those theories, and provide insight into IL properties and intermolecular interactions.

In spite of the general lack of success in finding correlations of ced_{IP} to other IL properties, several positive linear correlations have been found. The excellent linear correlation between two variables

Table 6. Summary of the challenges still remaining for intermolecular interactions of ILs.

experiments/calculations needed	ILs	information that could be accessed about intermolecular interactions of ILs
high sensitivity MS to determine ionic vapour composition at $T = 298$ K	any ILs	Calculations have suggested that neutral ion pairs are not the most favoured ionic vapour composition at $T = 298$ K. Such data are needed to have complete confidence in extrapolation of $\Delta_{vap}H$ data to $T = 298$ K.
Knudsen effusion MS to determine ionic vapour composition	any ILs apart from $[C_nC_1Im][NTf_2]$; ILs expected to have low $\Delta_{vap}H$ and high thermal stability would be good candidates (perhaps $[C_2C_1Im][FAP]$)	To demonstrate that the equilibrium ionic vapour composition of ILs (other than $[C_nC_1Im][NTf_2]$) is neutral ion pairs. Langmuir vaporization studies for a wide range of ILs strongly suggest that the equilibrium ionic vapour composition for all ILs is neutral ion pairs; however, no experimental has been recorded.
Knudsen effusion $\Delta_{vap}H$	any ILs apart from $[C_nC_1Im][NTf_2]$ for which $\Delta_{vap}H$ has already been measured using Langmuir vaporization; ILs expected to have low $\Delta_{vap}H$ and high thermal stability would be good candidates (perhaps $[C_2C_1Im][FAP]$)	To demonstrate that measuring $\Delta_{vap}H$ using the non-equilibrium Langmuir gives the same $\Delta_{vap}H$ values as the Knudsen effusion method, i.e. that there is no significant kinetic effect for Langmuir vaporization for ILs other than $[C_nC_1Im][NTf_2]$.
$\Delta_{vap}H$ at very different temperatures	any ILs apart from $[C_nC_1Im][NTf_2]$	To obtain $\Delta^g_lC_p$ directly from experiment for ILs other than $[C_nC_1Im][NTf_2]$. Such data would allow validation of $\Delta^g_lC_p$ values from other methods.
$\Delta_{vap}H$	ILs with small anions and long alkyl chains, e.g. $[C_8C_1Im][SCN]$	More data for such ILs has the potential to give significant insight into the underlying interactions that determine G_{IL}, and therefore, γ.
γ and ρ	any IL for which $\Delta_{vap}H$ has already been measured, but either γ or ρ has not been measured	To provide more ced_{IP} and G_{IL} data, which will allow further insight into intermolecular interactions without the need for further challenging measurements of $\Delta_{vap}H$.
$\Delta_{des}H$	any ILs	Delta;$_{des}H$(total) provides a measure of the total intermolecular interaction for an IL; hence, ced_{C+A} can be obtained. Currently $\Delta_{des}H$(total) data have only been published for $[C_2C_1Im][NTf_2]$. Having stated in §8.4 that ced_{IP} may be more useful than ced_{C+A} for correlating with other IL properties, it might appear that knowledge of ced_{C+A} is not useful; that is very much not the case. A key question is: are ced_{IP} versus ced_{C+A} linearly correlated? Do they essentially measure the same thing? Does size matter for ced_{C+A} as much as it does for ced_{IP}? How much does counterion affect $\Delta_{des}H$? Is desorption really enthalpically favourable for larger ion clusters?
calculations of $\Delta_{diss}H$(CA)	any ILs	How does $\Delta_{diss}H$(CA) vary with alkyl chain length? How does $\Delta_{diss}H$(CA) vary with the anion? Do electrostatic intermolecular interactions dominate $\Delta_{diss}H$(CA) for all ILs?
calculations of $\Delta_{des}H$(total) to get ced_{C+A}	any ILs	ced_{C+A} is very hard to measure experimentally, so insight into ced_{C+A} (and, therefore, the total intermolecular interactions for ILs) is needed.
calculations of vdW and electrostatic contributions to $\Delta_{des}H$(total) and, therefore, to ced_{C+A}	any ILs	Knowledge of the vdW and electrostatic contributions to IL total intermolecular interaction will give significant insight into the underlying reasons for trends. Do electrostatic intermolecular interactions dominate ced_{C+A} for all ILs?

derived solely from experimental data, ced_{IP} and V_m^{-1}, is an exciting development for ILs. Clearly, size matters when judging intermolecular interaction strengths for ILs. From this correlation, the ability to make *a priori* predictions of ced_{IP} without the need for synthesizing or characterizing an IL is a huge step forward in understanding IL intermolecular interactions, both in terms of being able to readily predict ced_{IP} in itself, but also giving the ability to test theories for ILs against other physical property data.

The good linear correlation between two variables derived solely from experimental data, ced_{IP} and G, is a further exciting development for ILs. This correlation gives significant insight into IL intermolecular interactions. However, further insight could be gained if more data were available for ced_{IP} and G, particularly for ILs with long alkyl chains and small anions.

ILs have very strong intermolecular interactions relative to most molecular liquids, as evidenced by the very large ced_{C+A} value, presented here for the first time. Electrostatic intermolecular interactions dominate for ILs, as might be expected for liquids composed solely of ions.

ILs are not involatile solely due to their ionic nature, and therefore, due to strong electrostatic interactions. Their vapour composition—neutral ions pairs—and their relatively large size (giving considerable vdW intermolecular interactions) contribute greatly too.

Data accessibility. All data used in this publication is available in the literature. A summary of the data used is accessible in the electronic supplementary material.

Authors' contributions. K.R.J.L. wrote the manuscript and gives final approval for publication.

Competing interests. I declare I have no competing interests.

Funding. K.R.J.L. is funded by the Royal Society.

Acknowledgements. K.R.J.L. acknowledges Imperial College London for the award of a Junior Research Fellowship and the Royal Society for the award of a University Research Fellowship. K.R.J.L. acknowledges Alasdair Taylor, Tom Welton, Yizhak Marcus, Richard Fogarty and Patricia Hunt for helpful discussion.

References

1. Wasserscheid P, Welton T (eds). 2008 *Ionic liquids in synthesis*, 2nd edn. Weinheim, Germany: Wiley-VCH.
2. Plechkova NV, Seddon KR. 2008 Applications of ionic liquids in the chemical industry. *Chem. Soc. Rev.* **37**, 123–150. (doi:10.1039/b006677j)
3. Hallett JP, Welton T. 2011 Room-temperature ionic liquids: solvents for synthesis and catalysis. 2. *Chem. Rev.* **111**, 3508–3576. (doi:10.1021/cr1003248)
4. Brandt A, Gräsvik J, Hallett JP, Welton T. 2013 Deconstruction of lignocellulosic biomass with ionic liquids. *Green Chem.* **15**, 550–583. (doi:10.1039/c2gc36364j)
5. MacFarlane DR *et al.* 2014 Energy applications of ionic liquids. *Energy Environ. Sci.* **7**, 232–250. (doi:10.1039/c3ee42099j)
6. Zhang XP, Zhang XC, Dong HF, Zhao ZJ, Zhang SJ, Huang Y. 2012 Carbon capture with ionic liquids: overview and progress. *Energy Environ. Sci.* **5**, 6668–6681. (doi:10.1039/c2ee21152a)
7. Zhou F, Liang YM, Liu WM. 2009 Ionic liquid lubricants: designed chemistry for engineering applications. *Chem. Soc. Rev.* **38**, 2590–2599. (doi:10.1039/b817899m)
8. Sun XQ, Luo HM, Dai S. 2012 Ionic liquids-based extraction: a promising strategy for the advanced nuclear fuel cycle. *Chem. Rev.* **112**, 2100–2128. (doi:10.1021/cr200193x)
9. Ho TD, Zhang C, Hantao LW, Anderson JL. 2014 Ionic liquids in analytical chemistry: fundamentals, advances, and perspectives. *Anal. Chem.* **86**, 262–285. (doi:10.1021/ac4035554)
10. Zhang SG, Zhang QH, Zhang Y, Chen ZJ, Watanabe M, Deng YQ. 2016 Beyond solvents and electrolytes: ionic liquids-based advanced functional materials. *Prog. Mater. Sci.* **77**, 80–124. (doi:10.1016/j.pmatsci.2015.10.001)
11. Gordon JE. 1975 *The organic chemistry of electrolyte solutions*. New York, NY: Wiley-Interscience.
12. Barton AFM. 1982 The application of cohesion parameters to wetting and adhesion—a review. *J. Adhes.* **14**, 33–62. (doi:10.1080/00218468208073199)
13. Evans DF. 1988 Self-organization of amphiphiles. *Langmuir.* **4**, 3–12. (doi:10.1021/la00079a002)
14. Evans DF, Wennerström H. 1999 *The colloidal domain: where physics, chemistry and biology meet engineering*, 2nd edn. New York, NY: Wiley-Blackwell.
15. Barton AFM. 1975 Solubility parameters. *Chem. Rev.* **75**, 731–753. (doi:10.1021/cr60298a003)
16. Kincaid JF, Eyring H, Stearn AE. 1941 The theory of absolute reaction rates and its application to viscosity and diffusion in the liquid state. *Chem. Rev.* **28**, 301–365. (doi:10.1021/cr60090a005)
17. Grunberg L, Nissan AH. 1949 The energies of vaporisation, viscosity and cohesion and the structure of liquids. *Trans. Faraday Soc.* **45**, 125–137. (10.1039/TF9494500125)
18. Harrap BS, Heymann E. 1951 Theories of viscosity applied to ionic liquids. *Chem. Rev.* **48**, 45–124. (doi:10.1021/cr60149a003)
19. Van Zeggeren F. 1956 The relation between activation energy of the viscosity and heat of vaporization for molten salts. *Can. J. Chem.-Rev. Can. Chim.* **34**, 1512–1514. (doi:10.1139/v56-196)
20. Burt R, Birkett G, Salanne M, Zhao XS. 2016 Molecular dynamics simulations of the influence of drop size and surface potential on the contact angle of ionic-liquid droplets. *J. Phys. Chem. C.* **120**, 15 244–15 250. (doi:10.1021/acs.jpcc.6b04696)
21. Merlet C, Rotenberg B, Madden PA, Taberna PL, Simon P, Gogotsi Y, Salanne M. 2012 On the molecular origin of supercapacitance in nanoporous carbon electrodes. *Nat. Mater.* **11**, 306–310. (doi:10.1038/nmat3260)
22. Hu YF, Liu ZC, Xu CM, Zhang XM. 2011 The molecular characteristics dominating the solubility of gases in ionic liquids. *Chem. Soc. Rev.* **40**, 3802–3823. (doi:10.1039/c0cs00006j)
23. Esperança JMSS, Canongia Lopes JN, Tariq M, Santos LMNBF, Magee JW, Rebelo LPN. 2010 Volatility of aprotic ionic liquids—a review. *J. Chem. Eng. Data* **55**, 3–12. (doi:10.1021/je900458w)
24. Rebelo LPN, Canongia Lopes JN, Esperança JMSS, Filipe E. 2005 On the critical temperature, normal boiling point, and vapor pressure of ionic liquids. *J. Phys. Chem. B* **109**, 6040–6043. (doi:10.1021/jp050430h)
25. Ueno K, Tokuda H, Watanabe M. 2010 Ionicity in ionic liquids: correlation with ionic structure and physicochemical properties. *Phys. Chem. Chem. Phys.* **12**, 1649–1658. (doi:10.1039/B921462N)
26. Veldhorst AA, Faria LFO, Ribeiro MCC. 2016 Local solvent properties of imidazolium-based ionic liquids. *J. Mol. Liq.* **223**, 283–288. (doi:10.1016/j.molliq.2016.08.044)
27. Freemantle M. 2009 *Introduction to ionic liquids*. Cambridge, UK: Royal Society of Chemistry.
28. Dack MRJ. 1975 Importance of solvent internal-pressure and cohesion to solution phenomena. *Chem. Soc. Rev.* **4**, 211–229. (doi:10.1039/cs9750400211)
29. Marcus Y. 1993 The properties of organic liquids that are relevant to their use as solvating solvents.

Chem. Soc. Rev. **22**, 409–416. (doi:10.1039/cs9932200409)

30. Reichardt C. 1994 Solvatochromic dyes as solvent polarity indicators. *Chem. Rev.* **94**, 2319–2358. (doi:10.1021/cr00032a005)
31. Heym F, Etzold BJM, Kern C, Jess A. 2011 Analysis of evaporation and thermal decomposition of ionic liquids by thermogravimetrical analysis at ambient pressure and high vacuum. *Green Chem.* **13**, 1453–1466. (doi:10.1039/c0gc00876a)
32. Marcus Y. 1998 *The properties of solvents*. Chichester, UK: Wiley.
33. Saecker ME, Nathanson GM. 1994 Collisions of protic and aprotic gases with a perfluorinated liquid. *J. Chem. Phys.* **100**, 3999–4005. (doi:10.1063/1.466333)
34. Harkins WD, Cheng YC. 1921 The orientation of molecules in surfaces. VI. Cohesion, adhesion, tensile strength, tensile energy, negative surface energy, interfacial tension, and molecular attraction. *J. Am. Chem. Soc.* **43**, 35–53. (doi:10.1021/ja01434a)
35. Bowden ST. 1955 Variation of surface tension and heat of vaporization with temperature. *J. Chem. Phys.* **23**, 2454–2455. (doi:10.1063/1.1741920)
36. Grosse AV. 1964 The relationship between surface tension and energy of liquid metals and their heat of vaporization at the melting point. *J. Inorg. Nucl. Chem.* **26**, 1349–1361. (doi:10.1016/0022-1902(64)80114-7)
37. Abdulnur SF. 1976 Relation of heat of vaporization to surface-tension for liquids of nonpolar spherical molecules. *J. Am. Chem. Soc.* **98**, 4039–4043. (doi:10.1021/ja00430a003)
38. Keeney M, Heicklen J. 1979 Surface-tension and the heat of vaporization: a simple empirical correlation. *J. Inorg. Nucl. Chem.* **41**, 1755–1758. (doi:10.1016/0022-1902(79)80118-9)
39. Becher P. 1972 Calculation of cohesive energy density from surface-tension of liquids. *J. Colloid Interface Sci.* **38**, 291–293. (doi:10.1016/0021-9797(72)90245-7)
40. Greaves TL, Drummond CJ. 2013 Solvent nanostructure, the solvophobic effect and amphiphile self-assembly in ionic liquids. *Chem. Soc. Rev.* **42**, 1096–1120. (doi:10.1039/c2cs35339c)
41. Wijaya EC, Greaves TL, Drummond CJ. 2013 Linking molecular/ion structure, solvent mesostructure, the solvophobic effect and the ability of amphiphiles to self-assemble in non-aqueous liquids. *Faraday Discuss.* **167**, 191–215. (doi:10.1039/c3fd00077j)
42. Greaves TL, Drummond CJ. 2008 Ionic liquids as amphiphile self-assembly media. *Chem. Soc. Rev.* **37**, 1709–1726. (doi:10.1039/b801395k)
43. Sedov IA, Solomonov BN. 2016 Thermodynamic description of the solvophobic effect in ionic liquids. *Fluid Phase Equilib.* **425**, 9–14. (doi:10.1016/j.fluid.2016.05.003)
44. Greaves TL, Drummond CJ. 2008 Protic ionic liquids: properties and applications. *Chem. Rev.* **108**, 206–237. (doi:10.1021/cr068040u)
45. Greaves TL, Drummond CJ. 2015 Protic ionic liquids: evolving structure-property relationships and expanding applications. *Chem. Rev.* **115**, 11 379–11 448. (doi:10.1021/acs.chemrev.5b00158)
46. Marcus Y. 1992 The structuredness of solvents. *J. Solut. Chem.* **21**, 1217–1230. (doi:10.1007/bf00667218)
47. Yang LX, Adam C, Cockroft SL. 2015 Quantifying solvophobic effects in nonpolar cohesive interactions. *J. Am. Chem. Soc.* **137**, 10 084–10 087. (doi:10.1021/jacs.5b05736)
48. Kamlet MJ, Carr PW, Taft RW, Abraham MH. 1981 Linear solvation energy relationships. 13. Relationship between the Hildebrand solubility parameter, delta-h, and the solvatochromic parameter, pi-star. *J. Am. Chem. Soc.* **103**, 6062–6066. (doi:10.1021/ja00410a013)
49. Hansen CM. 2007 *Hansen solubility parameters: a user's handbook*, 2nd edn. Boca Raton, FL: CRC Press.
50. Mutelet F, Butet V, Jaubert JN. 2005 Application of inverse gas chromatography and regular solution theory for characterization of ionic liquids. *Ind. Eng. Chem. Res.* **44**, 4120–4127. (doi:10.1021/ie048806l)
51. Ewell RH, Eyring H. 1937 Theory of viscosity of liquids as a function of temperature and pressure. *J. Chem. Phys.* **5**, 726–736. (doi:10.1063/1.1750108)
52. Xu W, Cooper EI, Angell CA. 2003 Ionic liquids: ion mobilities, glass temperatures, and fragilities. *J. Phys. Chem. B* **107**, 6170–6178. (doi:10.1021/jp0275894)
53. Barton AFM. 1991 *CRC handbook of solubility parameters and other cohesion parameters*, 2nd edn: Boca Raton, FL: CRC Press.
54. Marcus Y. 2013 Internal pressure of liquids and solutions. *Chem. Rev.* **113**, 6536–6551. (doi:10.1021/cr3004423)
55. Kolbeck C, Lehmann J, Lovelock KRJ, Cremer T, Paape N, Wasserscheid P, Fröba AP, Maier F, Steinrück HP. 2010 Density and surface tension of ionic liquids. *J. Phys. Chem. B* **114**, 17 025–17 036. (doi:10.1021/jp1068413)
56. Zaitsau DH, Kabo GJ, Strechan AA, Paulechka YU, Tschersich A, Verevkin SP, Heintz A. 2006 Experimental vapor pressures of 1-alkyl-3-methylimidazolium bis(trifluoromethylsulfonyl) imides and a correlation scheme for estimation of vaporization enthalpies of ionic liquids. *J. Phys. Chem. A* **110**, 7303–7306. (doi:10.1021/jp060896f)
57. Lovelock KRJ, Deyko A, Licence P, Jones RG. 2010 Vaporisation of an ionic liquid near room temperature. *Phys. Chem. Chem. Phys.* **12**, 8893–8901. (doi:10.1039/c004197a)
58. Seddon KR. 1997 Ionic liquids for clean technology. *J. Chem. Technol. Biotechnol.* **68**, 351–356. (doi:10.1002/(SICI)1097-4660(199704)68:4<351::AID-JCTB613>3.0.CO;2-4)
59. Earle MJ, Seddon KR. 2000 Ionic liquids: green solvents for the future. *Pure Appl. Chem.* **72**, 1391–1398. (doi:10.1351/pac200072071391)
60. Rogers RD, Seddon KR. 2003 Ionic liquids—solvents of the future? *Science* **302**, 792–793. (doi:10.1126/science.1090313)
61. Earle MJ, Esperança JMSS, Gilea MA, Canongia Lopes JN, Rebelo LPN, Magee JW, Seddon KR, Widegren JA. 2006 The distillation and volatility of ionic liquids. *Nature* **439**, 831–834. (doi:10.1038/nature04451)
62. Widegren JA, Wang YM, Henderson WA, Magee JW. 2007 Relative volatilities of ionic liquids by vacuum distillation of mixtures. *J. Phys. Chem. B* **111**, 8959–8964. (doi:10.1021/jp072964j)
63. Taylor AW, Lovelock KRJ, Deyko A, Licence P, Jones RG. 2010 High vacuum distillation of ionic liquids and separation of ionic liquid mixtures. *Phys. Chem. Chem. Phys.* **12**, 1772–1783. (doi:10.1039/B920931J)
64. Heym F, Etzold BJM, Kern C, Jess A. 2010 An improved method to measure the rate of vaporisation and thermal decomposition of high boiling organic and ionic liquids by thermogravimetrical analysis. *Phys. Chem. Chem. Phys.* **12**, 12 089–12 100. (doi:10.1039/c0cp00097c)
65. Heym F, Korth W, Thiessen J, Kern C, Jess A. 2015 Evaporation and decomposition behavior of pure and supported ionic liquids under thermal stress. *Chem. Ing. Tech.* **87**, 791–802. (doi:10.1002/cite.201400139)
66. Leal JP, Esperança JMSS, da Piedade MEM, Canongia Lopes JN, Rebelo LPN, Seddon KR. 2007 The nature of ionic liquids in the gas phase. *J. Phys. Chem. A* **111**, 6176–6182. (doi:10.1021/jp073006k)
67. Horikawa M, Akai N, Kawai A, Shibuya K. 2014 Vaporization of protic ionic liquids studied by matrix-isolation Fourier transform infrared spectroscopy. *J. Phys. Chem. A* **118**, 3280–3287. (doi:10.1021/jp501784w)
68. Ribeiro FMS, Lima CFRAC, Vaz ICM, Rodrigues ASMC, Sapei E, Melo A, Silva AMS, Santos LMNBF. 2017 Vaporization of protic ionic liquids derived from organic superbases and short carboxylic acids. *Phys. Chem. Chem. Phys.* **19**, 16 693–16 701. (doi:10.1039/c7cp02023f)
69. Reid JESJ, Agapito F, Bernardes CES, Martins F, Walker AJ, Shimizu S, da Piedade MEM. 2017 Structure–property relationships in protic ionic liquids: a thermochemical study. *Phys. Chem. Chem. Phys.* **19**, 19 928–19 936. (doi:10.1039/C7CP02230A)
70. Wasserscheid P. 2006 Chemistry—volatile times for ionic liquids. *Nature* **439**, 797. (doi:10.1038/439797a)
71. Armstrong JP, Hurst C, Jones RG, Licence P, Lovelock KRJ, Satterley CJ, Villar-Garcia IJ. 2007 Vapourisation of ionic liquids. *Phys. Chem. Chem. Phys.* **9**, 982–990. (doi:10.1039/B615137J)
72. Emel'yanenko VN, Verevkin SP, Heintz A, Corfield JA, Deyko A, Lovelock KRJ, Licence P, Jones RG. 2008 Pyrrolidinium-based ionic liquids. 1-butyl-1-methyl pyrrolidinium dicyanoamide: thermochemical measurement, mass spectrometry, and ab initio calculations. *J. Phys. Chem. B* **112**, 11 734–11 742. (doi:10.1021/jp803238t)
73. Deyko A *et al.* 2009 Measuring and predicting delta H-vap(298) values of ionic liquids. *Phys. Chem. Chem. Phys.* **11**, 8544–8555. (doi:10.1039/b908209c)
74. Deyko A, Lovelock KRJ, Licence P, Jones RG. 2011 The vapour of imidazolium-based ionic liquids: a mass spectrometry study. *Phys. Chem. Chem. Phys.* **13**, 16 841–16 850. (doi:10.1039/c1cp21821b)
75. Deyko A, Hessey SG, Licence P, Chernikova EA, Krasovskiy VG, Kustov LM, Jones RG. 2012 The enthalpies of vaporisation of ionic liquids: new measurements and predictions. *Phys. Chem. Chem. Phys.* **14**, 3181–3193. (doi:10.1039/c2cp23705a)
76. Hessey SG, Jones RG. 2013 On the evaporation, bonding, and adsorbate capture of an ionic liquid on Au(111). *Chem. Sci.* **4**, 2519–2529. (doi:10.1039/c3sc00072a)
77. Lovelock KRJ, Armstrong JP, Licence P, Jones RG. 2014 Vaporisation and thermal decomposition of dialkylimidazolium halide ion ionic liquids. *Phys.*

Chem. Chem. Phys. **16**, 1339–1353. (doi:10.1039/c3cp52950a)

78. Gross JH. 2008 Molecular ions of ionic liquids in the gas phase. *J. Am. Soc. Mass Spectrom.* **19**, 1347–1352. (doi:10.1016/j.jasms.2008.06.002)
79. Strasser D, Goulay F, Kelkar MS, Maginn EJ, Leone SR. 2007 Photoelectron spectrum of isolated ion-pairs in ionic liquid vapor. *J. Phys. Chem. A* **111**, 3191–3195. (doi:10.1021/jp071323l)
80. Chambreau SD, Vaghjiani GL, To A, Koh C, Strasser D, Kostko O, Leone SR. 2010 Heats of vaporization of room temperature ionic liquids by tunable vacuum ultraviolet photoionization. *J. Phys. Chem. B* **114**, 1361–1367. (doi:10.1021/jp909423m)
81. Strasser D, Goulay F, Belau L, Kostko O, Koh C, Chambreau SD, Vaghjiani GL, Ahmed M, Leone SR. 2010 Tunable wavelength soft photoionization of ionic liquid vapors. *J. Phys. Chem. A* **114**, 879–883. (doi:10.1021/jp909727f)
82. Chambreau SD, Vaghjiani GL, Koh CJ, Golan A, Leone SR. 2012 Ultraviolet photoionization efficiency of the vaporized ionic liquid 1-butyl-3-methylimidazolium tricyanomethanide: direct detection of the intact ion pair. *J. Phys. Chem. Lett.* **3**, 2910–2914. (doi:10.1021/jz301242w)
83. Koh CJ, Leone SR. 2012 Simultaneous ion-pair photodissociation and dissociative ionization of an ionic liquid: velocity map imaging of vacuum-ultraviolet-excited 1-ethyl-3-methylimidazolium bis(trifluoromethylsulfonyl)imide. *Mol. Phys.* **110**, 1705–1712. (doi:10.1080/00268976.2012.673019)
84. Obi EI, Leavitt CM, Raston PL, Moradi CP, Flynn SD, Vaghjiani GL, Boatz JA, Chambreau SD, Douberly GE. 2013 Helium nanodroplet isolation and infrared spectroscopy of the isolated ion-pair 1-ethyl-3-methylimidazolium bis(trifluoromethylsulfonyl) imide. *J. Phys. Chem. A* **117**, 9047–9056. (doi:10.1021/jp4078322)
85. Cooper R, Zolot AM, Boatz JA, Sporleder DP, Stearns JA. 2013 IR and UV spectroscopy of vapor-phase jet-cooled ionic liquid emim (+) Tf2N (-): ion pair structure and photodissociation dynamics. *J. Phys. Chem. A* **117**, 12 419–12 428. (doi:10.1021/jp409670n)
86. Chilingarov NS *et al.* 2015 Mass spectrometric studies of 1-ethyl-3-methylimidazolium and 1-propyl-2,3-dimethylimidazolium bis(trifluoromethyl)-sulfonylimides. *Rapid Commun. Mass Spectrom.* **29**, 1227–1232. (doi:10.1002/rcm.7214)
87. Dunaev AM, Motalov VB, Kudin LS, Butman MF. 2016 Molecular and ionic composition of saturated vapor over EMImNTf(2) ionic liquid. *J. Mol. Liq.* **219**, 599–601. (doi:10.1016/j.molliq.2016.03.074)
88. Brunetti B, Ciccioli A, Gigli G, Lapi A, Misceo N, Tanzi L, Ciprioti SV. 2014 Vaporization of the prototypical ionic liquid BMImNTf(2) under equilibrium conditions: a multitechnique study. *Phys. Chem. Chem. Phys.* **16**, 15 653–15 661. (doi:10.1039/c4cp01673d)
89. Tolstogouzov A, Bardi U, Nishikawa O, Taniguchi M. 2008 Study on imidazolium-based ionic liquids with scanning atom probe and Knudsen effusion mass spectrometry. *Surf. Interface Anal.* **40**, 1614–1618. (doi:10.1002/sia.2906)
90. Chambreau SD, Boatz JA, Vaghjiani GL, Koh C, Kostko O, Golan A, Leone SR. 2012 Thermal decomposition mechanism of 1-ethyl-3-methylimidazolium bromide ionic liquid. *J. Phys. Chem. A* **116**, 5867–5876. (doi:10.1021/jp209389d)
91. Dunaev AM, Motalov VB, Kudin LS, Butman MF. 2016 Thermodynamic properties of the ionic vapor species over EMImNTf(2) ionic liquid studied by Knudsen effusion mass spectrometry. *J. Mol. Liq.* **223**, 407–411. (doi:10.1016/j.molliq.2016.08.060)
92. Neto BAD, Meurer EC, Galaverna R, Bythell BJ, Dupont J, Cooks RG, Eberlin MN. 2012 Vapors from ionic liquids: reconciling simulations with mass spectrometric data. *J. Phys. Chem. Lett.* **3**, 3435–3441. (doi:10.1021/jz301608c)
93. Berkowitz J, Chupka WA. 1958 Polymeric gaseous molecules in the vaporization of alkali halides. *J. Chem. Phys.* **29**, 653–657. (doi:10.1063/1.1744555)
94. Lovelock KRJ, Deyko A, Corfield JA, Gooden PN, Licence P, Jones RG. 2009 Vaporisation of a dicationic ionic liquid. *Chemphyschem.* **10**, 337–340. (doi:10.1002/cphc.200800690)
95. Vitorino J, Leal JP, Licence P, Lovelock KRJ, Gooden PN, da Piedade MEM, Shimizu K, Rebelo LPN, Canongia Lopes JN. 2010 Vaporisation of a dicationic ionic liquid revisited. *Chemphyschem.* **11**, 3673–3677. (doi:10.1002/cphc.201000723)
96. Zaitsau DH, Yermalayeu AV, Emel'yanenko VN, Butler S, Schubert T, Verevkin SP. 2016 Thermodynamics of imidazolium-based ionic liquids containing PF6 Anions. *J. Phys. Chem. B* **120**, 7949–7957. (doi:10.1021/acs.jpcb.6b06081)
97. Ballone P, Pinilla C, Kohanoff J, Del Pópolo MG. 2007 Neutral and charged 1-butyl-3-methylimidazolium triflate clusters: equilibrium concentration in the vapor phase and thermal properties of nanometric droplets. *J. Phys. Chem. B* **111**, 4938–4950. (doi:10.1021/jp067484r)
98. Kelkar MS, Maginn EJ. 2007 Calculating the enthalpy of vaporization for ionic liquid clusters. *J. Phys. Chem. B* **111**, 9424–9427. (doi:10.1021/jp073253o)
99. Rai N, Maginn EJ. 2011 Vapor-liquid coexistence and critical behavior of ionic liquids via molecular simulations. *J. Phys. Chem. Lett.* **2**, 1439–1443. (doi:10.1021/jz200526z)
100. Rai N, Maginn EJ. 2012 Critical behaviour and vapour-liquid coexistence of 1-alkyl-3-methylimidazolium bis(trifluoromethylsulfonyl) amide ionic liquids via Monte Carlo simulations. *Faraday Discuss.* **154**, 53–69. (doi:10.1039/c1fd00090j)
101. Chaban VV, Prezhdo OV. 2012 Ionic vapor: what does it consist of? *J. Phys. Chem. Lett.* **3**, 1657–1662. (doi:10.1021/jz300405q)
102. Chaban VV, Prezhdo OV. 2016 Ionic vapor composition in pyridinium-based ionic liquids. *J. Phys. Chem. B* **120**, 4661–4667. (doi:10.1021/acs.jpcb.6b03130)
103. Preiss U, Verevkin SP, Koslowski T, Krossing I. 2011 Going full circle: phase-transition thermodynamics of ionic liquids. *Chem.-Eur. J.* **17**, 6508–6517. (doi:10.1002/chem.201003150)
104. McDaniel JG, Choi E, Son CY, Schmidt JR, Yethiraj A. 2016 Ab initio force fields for imidazolium-based ionic liquids. *J. Phys. Chem. B* **120**, 7024–7036. (doi:10.1021/acs.jpcb.6b05328)
105. Lui MY, Crowhurst L, Hallett JP, Hunt PA, Niedermeyer H, Welton T. 2011 Salts dissolved in salts: ionic liquid mixtures. *Chem. Sci.* **2**, 1491–1496. (doi:10.1039/c1sc00227a)
106. Ahrenberg M, Brinckmann M, Schmelzer JWP, Beck M, Schmidt C, Kessler O, Kragl U, Verevkin SP, Schick C. 2014 Determination of volatility of ionic liquids at the nanoscale by means of ultra-fast scanning calorimetry. *Phys. Chem. Chem. Phys.* **16**, 2971–2980. (doi:10.1039/c3cp54325k)
107. Ahrenberg M, Beck M, Neise C, Kessler O, Kragl U, Verevkin SP, Schick C. 2016 Vapor pressure of ionic liquids at low temperatures from AC-chip-calorimetry. *Phys. Chem. Chem. Phys.* **18**, 21 381–21 390. (doi:10.1039/c6cp01948j)
108. Luo HM, Baker GA, Dai S. 2008 Isothermogravimetric determination of the enthalpies of vaporization of 1-alkyl-3-methylimidazolium ionic liquids. *J. Phys. Chem. B* **112**, 10 077–10 081. (doi:10.1021/jp805340f)
109. Verevkin SP, Ralys RV, Zaitsau DH, Emel'yanenko VN, Schick C. 2012 Express thermo-gravimetric method for the vaporization enthalpies appraisal for very low volatile molecular and ionic compounds. *Thermochim. Acta* **538**, 55–62. (doi:10.1016/j.tca.2012.03.018)
110. Verevkin SP, Zaitsau DH, Emel'yanenko VN, Ralys RV, Yermalayeu AV, Schick C. 2012 Vaporization enthalpies of imidazolium based ionic liquids: a thermogravimetric study of the alkyl chain length dependence. *J. Chem. Thermodyn.* **54**, 433–437. (doi:10.1016/j.jct.2012.05.029)
111. Verevkin SP *et al.* 2013 Making sense of enthalpy of vaporization trends for ionic liquids: new experimental and simulation data show a simple linear relationship and help reconcile previous data. *J. Phys. Chem. B* **117**, 6473–6486. (doi:10.1021/jp311429r)
112. Zaitsau DH, Yermalayeu AV, Emel'yanenko VN, Heintz A, Verevkin SP, Schick C, Berdzinski S, Strehmel V. 2014 Structure-property relationships in ILs: vaporization enthalpies of pyrrolidinium based ionic liquids. *J. Mol. Liq.* **192**, 171–176. (doi:10.1016/j.molliq.2013.07.018)
113. Seeberger A, Andresen AK, Jess A. 2009 Prediction of long-term stability of ionic liquids at elevated temperatures by means of non-isothermal thermogravimetrical analysis. *Phys. Chem. Chem. Phys.* **11**, 9375–9381. (10.1039/B909624H)
114. Zaitsau DH, Yermalayeu AV, Emel'yanenko VN, Schick C, Verevkin SP, Samarov AA, Schlenk S, Wasserscheid P. 2013 Structure-property relations in ionic liquids: 1,2,3-trimethyl-imidazolium and 1,2,3-trimethyl-benzimidazolium bis-(trifluorsulfonyl)imide. *Z. Phys. Chemie-Int. J. Res. Phys. Chem. Chem. Phys.* **227**, 205–215. (doi:10.1524/zpch.2013.0312)
115. Zaitsau DH, Yermalayeu AV, Verevkin SP, Bara JE, Stanton AD. 2013 Structure-property relationships in ionic liquids: a study of the influence of N(1) ether and C(2) methyl substituents on the vaporization enthalpies of innidazolium-based ionic liquids. *Ind. Eng. Chem. Res.* **52**, 16 615–16 621. (doi:10.1021/ie402664c)
116. Zaitsau DH, Yermalayeu AV, Verevkin SP, Bara JE, Wallace DA. 2015 Structure-property relationships in ionic liquids: chain length dependence of the vaporization enthalpies of imidazolium-based ionic liquids with fluorinated substituents. *Thermochim. Acta* **622**, 38–43. (doi:10.1016/j.tca.2015.04.021)
117. Emel'yanenko VN, Verevkin SP, Heintz A. 2007 The gaseous enthalpy of formation of the ionic liquid

1-butyl-3-methylimidazolium dicyanamide from combustion calorimetry, vapor pressure measurements, and ab initio calculations. *J. Am. Chem. Soc.* **129**, 3930–3937. (doi:10.1021/ja0679174)

118. Wang CM, Luo HM, Li HR, Dai S. 2010 Direct UV-spectroscopic measurement of selected ionic-liquid vapors. *Phys. Chem. Chem. Phys.* **12**, 7246–7250. (doi:10.1039/c001101k)
119. Verevkin SP, Zaitsau DH, Emelyanenko VN, Heintz A. 2011 A new method for the determination of vaporization enthalpies of ionic liquids at low temperatures. *J. Phys. Chem. B* **115**, 12 889–12 895. (doi:10.1021/jp207397v)
120. Zaitsau DH, Verevkin SP, Emel'yanenko VN, Heintz A. 2011 Vaporization enthalpies of imidazolium based ionic liquids: dependence on alkyl chain length. *Chemphyschem.* **12**, 3609–3613. (doi:10.1002/cphc.201100618)
121. Fumino K, Peppel T, Geppert-Rybczynska M, Zaitsau DH, Lehmann JK, Verevkin SP, Köckerling M, Ludwig R. 2011 The influence of hydrogen bonding on the physical properties of ionic liquids. *Phys. Chem. Chem. Phys.* **13**, 14 064–14 075. (doi:10.1039/c1cp20732f)
122. Emel'yanenko VN, Zaitsau DH, Verevkin SP, Heintz A, Voss K, Schulz A. 2011 Vaporization and formation enthalpies of 1-alkyl-3-methylimidazolium tricyanomethanides. *J. Phys. Chem. B* **115**, 11 712–11 717. (doi:10.1021/jp207335m)
123. Zaitsau DH, Fumino K, Emel'yanenko VN, Yermalayeu AV, Ludwig R, Verevkin SP. 2012 Structure-property relationships in ionic liquids: a study of the anion dependence in vaporization enthalpies of imidazolium-based ionic liquids. *Chemphyschem.* **13**, 1868–1876. (doi:10.1002/cphc.201100879)
124. Zaitsau DH, Yermalayeu AV, Emel'yanenko VN, Verevkin SP, Welz-Biermann U, Schubert T. 2012 Structure-property relationships in ILs: a study of the alkyl chain length dependence in vaporisation enthalpies of pyridinium based ionic liquids. *Sci. China-Chem.* **55**, 1525–1531. (doi:10.1007/s11426-012-4662-2)
125. Zaitsau DH, Varfolomeev MA, Verevkin SP, Stanton AD, Hindman MS, Bara JE. 2016 Structure-property relationships in ionic liquids: influence of branched and cyclic groups on vaporization enthalpies of imidazolium-based ILs. *J. Chem. Thermodyn.* **93**, 151–156. (doi:10.1016/j.jct.2015.09.033)
126. Zaitsau DH, Kaliner M, Lerch S, Strassner T, Emel'yanenko VN, Verevkin SP. 2017 Thermochemical properties of tunable aryl alkyl ionic liquids (TAAILs) based on phenyl-1H-imidazoles. *Z. Anorg. Allg. Chem.* **643**, 114–119. (doi:10.1002/zaac.201600333)
127. Zaitsau DH, Yermalayeu AV, Emel'yanenko VN, Schulz A, Verevkin SP. 2017 Thermochemistry of pyridinium based ionic liquids with tetrafluoroborate anion. *Z. Anorg. Allg. Chem.* **643**, 87–92. (doi:10.1002/zaac.201600335)
128. Yermalayeu AV, Zaitsau DH, Loor M, Schaumann J, Emel'yanenko VN, Schulz S, Verevkin SP. 2017 Imidazolium based ionic liquids: impact of the cation symmetry and alkyl chain length on the enthalpy of vaporization. *Z. Anorg. Allg. Chem.* **643**, 81–86. (doi:10.1002/zaac.201600332)
129. Rocha MAA *et al.* 2011 High-accuracy vapor pressure data of the extended [C(n)C(1)im][Ntf(2)] ionic liquid series: trend changes and structural shifts. *J. Phys. Chem. B* **115**, 10 919–10 926. (doi:10.1021/jp2049316)
130. Rocha MAA, Coutinho JAP, Santos LMNBF. 2012 Cation symmetry effect on the volatility of ionic liquids. *J. Phys. Chem. B* **116**, 10 922–10 927. (doi:10.1021/jp306937f)
131. Rocha MAA, Santos LMNBF. 2013 First volatility study of the 1-alkylpyridinium based ionic liquids by Knudsen effusion. *Chem. Phys. Lett.* **585**, 59–62. (doi:10.1016/j.cplett.2013.08.095)
132. Rocha MAA, Ribeiro FMS, Schröder B, Coutinho JAP, Santos LMNBF. 2014 Volatility study of $[C_1C_1im][NTf_2]$ and $[C_2C_3im][NTf_2]$ ionic liquids. *J. Chem. Thermodyn.* **68**, 317–321. (doi:10.1016/j.jct.2013.09.020)
133. Rocha MAA, Coutinho JAP, Santos LMNBF. 2014 Vapor pressures of 1,3-dialkylimidazolium bis(trifluoromethylsulfonyl)imide ionic liquids with long alkyl chains. *J. Chem. Phys.* **141**, 8. (doi:10.1063/1.4896704)
134. Vilas M, Rocha MAA, Fernandes AM, Tojo E, Santos LMNBF. 2015 Novel 2-alkyl-1-ethylpyridinium ionic liquids: synthesis, dissociation energies and volatility. *Phys. Chem. Chem. Phys.* **17**, 2560–2572. (doi:10.1039/c4cp05191b)
135. Paulechka E, Blokhin AV, Rodrigues ASMC, Rocha MAA, Santos LMNBF. 2016 Thermodynamics of long-chain 1-alkyl-3-methylimidazolium bis(trifluoromethanesulfonyl)imide ionic liquids. *J. Chem. Thermodyn.* **97**, 331–340. (doi:10.1016/j.jct.2016.02.009)
136. Yermalayeu AV, Zaitsau DH, Emel'yanenko VN, Verevkin SP. 2015 Thermochemistry of ammonium based ionic liquids: thiocyanates-experiments and computations. *J. Solut. Chem.* **44**, 754–768. (doi:10.1007/s10953-015-0316-2)
137. Paulechka YU. 2010 Heat capacity of room-temperature ionic liquids: a critical review. *J. Phys. Chem. Ref. Data* **39**, 23. (doi:10.1063/1.3463478)
138. Paulechka YU, Kabo GJ, Blokhin AV, Vydrov OA, Magee JW, Frenkel M. 2003 Thermodynamic properties of 1-butyl-3-methylimidazolium hexafluorophosphate in the ideal gas state. *J. Chem. Eng. Data* **48**, 457–462. (doi:10.1021/je025591i)
139. Paulechka YU, Kabo GJ, Emel'yanenko VN. 2008 Structure, conformations, vibrations, and ideal-gas properties of 1-alkyl-3-methylimidazolium bis(trifluoromethylsulfonyl)imide ionic pairs and constituent ions. *J. Phys. Chem. B* **112**, 15 708–15 717. (doi:10.1021/jp804607n)
140. Kabo GJ, Paulechka YU, Zaitsau DH, Firaha AS. 2015 Prediction of the enthalpies of vaporization for room-temperature ionic liquids: correlations and a substitution-based additive scheme. *Thermochim. Acta* **609**, 7–19. (doi:10.1016/j.tca.2015.04.013)
141. Taylor AW, Lovelock KRJ, Jones RG, Licence P. 2011 Borane-substituted imidazol-2-ylidenes: syntheses in vacuo. *Dalton Trans.* **40**, 1463–1470. (doi:10.1039/c0dt01240h)
142. Santos LMNBF, Canongia Lopes JN, Coutinho JAP, Esperança JMSS, Gomes LR, Marrucho IM, Rebelo LPN. 2007 Ionic liquids: first direct determination of their cohesive energy. *J. Am. Chem. Soc.* **129**, 284–285. (doi:10.1021/ja067427b)
143. Hong M, Liu RJ, Yang HX, Guan W, Tong J, Yang JZ. 2014 Determination of the vaporisation enthalpies and estimation of the polarity for 1-alkyl-3-methylimidazolium propionate {$[C_n$mim][Pro] ($n = 2, 3$)} ionic liquids. *J. Chem. Thermodyn.* **70**, 214–218. (doi:10.1016/j.jct.2013.11.004)
144. Clough MT, Geyer K, Hunt PA, Mertes J, Welton T. 2013 Thermal decomposition of carboxylate ionic liquids: trends and mechanisms. *Phys. Chem. Chem. Phys.* **15**, 20 480–20 495. (doi:10.1039/c3cp53648c)
145. Salgado J, Villanueva M, Parajo JJ, Fernandez J. 2013 Long-term thermal stability of five imidazolium ionic liquids. *J. Chem. Thermodyn.* **65**, 184–190. (doi:10.1016/j.jct.2013.05.049)
146. Villanueva M, Coronas A, Garcia J, Salgado J. 2013 Thermal stability of ionic liquids for their application as new absorbents. *Ind. Eng. Chem. Res.* **52**, 15 718–15 727. (doi:10.1021/ie401656e)
147. Verevkin SP, Zaitsau DH, Emel'yanenko VN, Ralys RV, Schick C, Geppert-Rybczyńska M, Jayaraman S, Maginn EJ. 2012 Benchmark values: thermochemistry of the ionic liquid [C4Py][Cl]. *Aust. J. Chem.* **65**, 1487–1490. (doi:10.1071/ch12314)
148. Kamavaram V, Reddy RG. 2008 Thermal stabilities of di-alkylimidazolium chloride ionic liquids. *Int. J. Therm. Sci.* **47**, 773–777. (doi:10.1016/j.ijthermalsci.2007.06.012)
149. Ogura T, Akai N, Kawai A, Shibuya K. 2013 Gas phase electronic absorption spectroscopy of room temperature ionic liquids: *N*-ethyl-3-methylpyridinium or 1-butyl-3-methylimidazolium cation with bis(trifluoromethylsulfonyl)amido anion. *Chem. Phys. Lett.* **555**, 110–114. (doi:10.1016/j.cplett.2012.10.075)
150. Zaitsau DH, Emel'yanenko VN, Stange P, Schick C, Verevkin SP, Ludwig R. 2016 Dispersion and hydrogen bonding rule: why the vaporization enthalpies of aprotic ionic liquids are significantly larger than those of protic ionic liquids. *Angew. Chem.-Int. Edit.* **55**, 11 682–11 686. (doi:10.1002/anie.201605633)
151. Paulechka YU, Zaitsau DH, Kabo GJ, Strechan AA. 2005 Vapor pressure and thermal stability of ionic liquid 1-butyl-3-methylimidazolium bis(trifluoromethylsulfonyl)amide. *Thermochim. Acta* **439**, 158–160. (doi:10.1016/j.tca.2005.08.035)
152. Rodrigues ASMC, Lima CFRAC, Coutinho JAP, Santos LMNBF. 2017 Nature of the C2-methylation effect on the properties of imidazolium ionic liquids. *Phys. Chem. Chem. Phys.* **19**, 5326–5332. (doi:10.1039/c6cp08451f)
153. Zaitsau DH, Paulechka YU, Kabo GJ. 2006 The kinetics of thermal decomposition of 1-butyl-3-methylimidazolium hexafluorophosphate. *J. Phys. Chem. A* **110**, 11 602–11 604. (doi:10.1021/jp064212f)
154. Köddermann T, Paschek D, Ludwig R. 2007 Molecular dynamic simulations of ionic liquids: a reliable description of structure, thermodynamics and dynamics. *Chemphyschem.* **8**, 2464–2470. (doi:10.1002/cphc.200700552)
155. Köddermann T, Paschek D, Ludwig R. 2008 Ionic liquids: dissecting the enthalpies of vaporization. *Chemphyschem.* **9**, 549–555. (doi:10.1002/cphc.200700814)
156. Shimizu K, Tariq M, Costa Gomes MF, Rebelo LPN, Canongia Lopes JN. 2010 Assessing the dispersive and electrostatic components of the cohesive energy or ionic liquids using molecular dynamics simulations and molar refraction data. *J. Phys. Chem. B* **114**, 5831–5834. (doi:10.1021/jp101910c)

157. Diedenhofen M, Klamt A, Marsh K, Schäfer A. 2007 Prediction of the vapor pressure and vaporization enthalpy of 1-n-alkyl-3-methylimidazolium-bis-(trifluoromethanesulfonyl) amide ionic liquids. *Phys. Chem. Chem. Phys.* **9**, 4653–4656. (doi:10.1039/B706728C)
158. Schröder B, Coutinho JAP. 2014 Predicting enthalpies of vaporization of aprotic ionic liquids with COSMO-RS. *Fluid Phase Equilib.* **370**, 24–33. (doi:10.1016/j.fluid.2014.02.026)
159. Fröba AP, Kremer H, Leipertz A. 2008 Density, refractive index, interfacial tension, and viscosity of ionic liquids EMIM EtSO4, EMIM NTf2, EMIM N(CN)(2), and OMA NTf2 in dependence on temperature at atmospheric pressure. *J. Phys. Chem. B* **112**, 12 420–12 430. (doi:10.1021/jp804319a)
160. Carvalho PJ, Freire MG, Marrucho IM, Queimada AJ, Coutinho JAP. 2008 Surface tensions for the 1-alkyl-3-methylimidazolium bis(trifluoromethylsulfonyl)imide ionic liquids. *J. Chem. Eng. Data* **53**, 1346–1350. (doi:10.1021/je800069z)
161. Esperança JMSS, Visak ZP, Plechkova NV, Seddon KR, Guedes HJR, Rebelo LPN. 2006 Density, speed of sound, and derived thermodynamic properties of ionic liquids over an extended pressure range. 4. $[C_3mim][NTf_2]$ and $[C_5mim][NTf_2]$. *J. Chem. Eng. Data* **51**, 2009–2015. (doi:10.1021/je060203o)
162. Gardas RL, Freire MG, Carvalho PJ, Marrucho IM, Fonseca IMA, Ferreira AGM, Coutinho JAP. 2007 $P\rho T$ measurements of imidazolium-based ionic liquids. *J. Chem. Eng. Data* **52**, 1881–1888. (doi:10.1021/je700205n)
163. Almeida HFD *et al.* 2014 Cation alkyl side chain length and symmetry effects on the surface tension of ionic liquids. *Langmuir* **30**, 6408–6418. (doi:10.1021/la501308q)
164. Fredlake CP, Crosthwaite JM, Hert DG, Aki S, Brennecke JF. 2004 Thermophysical properties of imidazolium-based ionic liquids. *J. Chem. Eng. Data* **49**, 954–964. (doi:10.1021/je034261a)
165. Fletcher SI, Sillars FB, Hudson NE, Hall PJ. 2010 Physical properties of selected ionic liquids for use as electrolytes and other industrial applications. *J. Chem. Eng. Data* **55**, 778–782. (doi:10.1021/je900405j)
166. Katsuta S, Shiozawa Y, Imai K, Kudo Y, Takeda Y. 2010 Stability of ion pairs of bis(trifluoromethanesulfonyl)amide-based ionic liquids in dichloromethane. *J. Chem. Eng. Data* **55**, 1588–1593. (doi:10.1021/je900694m)
167. Carvalho PJ, Neves C, Coutinho JAP. 2010 Surface tensions of bis(trifluoromethylsulfonyl)imide anion-based ionic liquids. *J. Chem. Eng. Data* **55**, 3807–3812. (doi:10.1021/je100253m)
168. Anderson JL, Ding RF, Ellern A, Armstrong DW. 2005 Structure and properties of high stability geminal dicationic ionic liquids. *J. Am. Chem. Soc.* **127**, 593–604. (doi:10.1021/ja046521u)
169. Chen ZJ, Huo YN, Cao J, Xu L, Zhang SG. 2016 Physicochemical properties of ether-functionalized ionic liquids: understanding their irregular variations with the ether chain length. *Ind. Eng. Chem. Res.* **55**, 11 589–11 596. (doi:10.1021/acs.iecr.6b02875)
170. Rocha MAA, Neves CMSS, Freire MG, Russina O, Triolo A, Coutinho JAP, Santos LMNBF. 2013 Alkylimidazolium based ionic liquids: impact of cation symmetry on their nanoscale structural organization. *J. Phys. Chem. B* **117**, 10 889–10 897. (doi:10.1021/jp406374a)
171. Rodrigues ASMC, Rocha MAA, Almeida HFD, Neves C, Lopes-da-Silva JA, Freire MG, Coutinho JAP, Santos LMNBF. 2015 Effect of the methylation and N-H acidic group on the physicochemical properties of imidazolium-based ionic liquids. *J. Phys. Chem. B* **119**, 8781–8792. (doi:10.1021/acs.jpcb.5b05354)
172. Gardas RL, Costa HF, Freire MG, Carvalho PJ, Marrucho IM, Fonseca IMA, Ferreira AGM, Coutinho JAP. 2008 Densities and derived thermodynamic properties of imidazolium-, pyridinium-, pyrrolidinium-, and piperidinium-based ionic liquids. *J. Chem. Eng. Data* **53**, 805–811. (doi:10.1021/je700670k)
173. Jin H, O'Hare B, Dong J, Arzhantsev S, Baker GA, Wishart JF, Benesi AJ, Maroncelli M. 2008 Physical properties of ionic liquids consisting of the 1-butyl-3-methylimidazolium cation with various anions and the bis(trifluoromethylsulfonyl)imide anion with various cations. *J. Phys. Chem. B* **112**, 81–92. (doi:10.1021/jp076462h)
174. Liu QS, Yang MA, Yan PF, Liu XM, Tan ZC, Welz-Biermann U. 2010 Density and surface tension of ionic liquids $[C_npy][NTf_2]$ (n=2, 4, 5). *J. Chem. Eng. Data* **55**, 4928–4930. (doi:10.1021/je100507n)
175. Shirota H, Mandai T, Fukazawa H, Kato T. 2011 Comparison between dicationic and monocationic ionic liquids: liquid density, thermal properties, surface tension, and shear viscosity. *J. Chem. Eng. Data* **56**, 2453–2459. (doi:10.1021/je2000183)
176. Tiago G, Restolho J, Forte A, Colaco R, Branco LC, Saramago B. 2015 Novel ionic liquids for interfacial and tribological applications. *Colloid Surf. A-Physicochem. Eng. Asp.* **472**, 1–8. (doi:10.1016/j.colsurfa.2015.02.030)
177. Bandres I, Royo FM, Gascon I, Castro M, Lafuente C. 2010 Anion influence on thermophysical properties of ionic liquids: 1-butylpyridinium tetrafluoroborate and 1-butylpyridinium triflate. *J. Phys. Chem. B* **114**, 3601–3607. (doi:10.1021/jp9120707)
178. Bandres I, Giner B, Artigas H, Royo FM, Lafuente C. 2008 Thermophysic comparative study of two isomeric pyridinium-based ionic liquids. *J. Phys. Chem. B* **112**, 3077–3084. (doi:10.1021/jp077259p)
179. Gómez E, González B, Calvar N, Tojo E, Domínguez A. 2006 Physical properties of pure 1-ethyl-3-methylimidazolium ethylsulfate and its binary mixtures with ethanol and water at several temperatures. *J. Chem. Eng. Data* **51**, 2096–2102. (doi:10.1021/je060228n)
180. Hasse B, Lehmann J, Assenbaum D, Wasserscheid P, Leipertz A, Fröba AP. 2009 Viscosity, interfacial tension, density, and refractive index of ionic liquids [EMIM][MeSO3], [EMIM][MeOHPO2], [EMIM][OcSO(4)], and [BBIM][NTf2] in dependence on temperature at atmospheric pressure. *J. Chem. Eng. Data* **54**, 2576–2583. (doi:10.1021/je900134z)
181. Wandschneider A, Lehmann JK, Heintz A. 2008 Surface tension and density of pure ionic liquids and some binary mixtures with 1-propanol and 1-butanol. *J. Chem. Eng. Data* **53**, 596–599. (doi:10.1021/je700621d)
182. Freire MG, Teles ARR, Rocha MAA, Schröder B, Neves CMSS, Carvalho PJ, Evtuguin DV, Santos LMNBF, Coutinho JAP. 2011 Thermophysical characterization of ionic liquids able to dissolve biomass. *J. Chem. Eng. Data* **56**, 4813–4822. (doi:10.1021/je200790q)
183. Almeida HFD, Teles ARR, Lopes-da-Silva JA, Freire MG, Coutinho JAP. 2012 Influence of the anion on the surface tension of 1-ethyl-3-methylimidazolium-based ionic liquids. *J. Chem. Thermodyn.* **54**, 49–54. (doi:10.1016/j.jct.2012.03.008)
184. Klomfar J, Součková M, Pátek J. 2009 Surface tension measurements for four 1-alkyl-3-methylimidazolium-based ionic liquids with hexafluorophosphate anion. *J. Chem. Eng. Data* **54**, 1389–1394. (doi:10.1021/je800895q)
185. Harris KR, Kanakubo M, Woolf LA. 2007 Temperature and pressure dependence of the viscosity of the ionic liquids 1-hexyl-3-methylimidazolium hexafluorophosphate and 1-butyl-3-methylimidazolium bis(trifluoromethylsulfonyl)imide. *J. Chem. Eng. Data* **52**, 1080–1085. (doi:10.1021/je700032n)
186. Domanska U, Krolikowska M, Krolikowski M. 2010 Phase behaviour and physico-chemical properties of the binary systems {1-ethyl-3-methylimidazolium thiocyanate, or 1-ethyl-3-methylimidazolium tosylate plus water, or plus an alcohol}. *Fluid Phase Equilib.* **294**, 72–83. (doi:10.1016/j.fluid.2010.01.020)
187. Kulkarni PS, Branco LC, Crespo JG, Nunes MC, Raymundo A, Afonso CAM. 2007 Comparison of physicochemical properties of new ionic liquids based on imidazolium, quaternary ammonium, and guanidinium cations. *Chem.-Eur. J.* **13**, 8478–8488. (doi:10.1002/chem.200700965)
188. Carrera GVSM, Afonso CAM, Branco LC. 2010 Interfacial properties, densities, and contact angles of task specific ionic liquids. *J. Chem. Eng. Data* **55**, 609–615. (doi:10.1021/je900502s)
189. Sanchez LG, Espel JR, Onink F, Meindersma GW, de Haan AB. 2009 Density, viscosity, and surface tension of synthesis grade imidazolium, pyridinium, and pyrrolidinium based room temperature ionic liquids. *J. Chem. Eng. Data* **54**, 2803–2812. (doi:10.1021/je800710p)
190. Koller TM, Schmid SR, Sachnov SJ, Rausch MH, Wasserscheid P, Fröba AP. 2014 Measurement and prediction of the thermal conductivity of tricyanomethanide- and tetracyanoborate-based imidazolium ionic liquids. *Int. J. Thermophys.* **35**, 195–217. (doi:10.1007/s10765-014-1617-1)
191. Koller TM, Rausch MH, Pohako-Esko K, Wasserscheid P, Fröba AP. 2015 Surface tension of tricyanomethanide- and tetracyanoborate-based imidazolium ionic liquids by using the pendant drop method. *J. Chem. Eng. Data* **60**, 2665–2673. (doi:10.1021/acs.jced.5b00303)
192. Koller TM, Rausch MH, Schulz PS, Berger M, Wasserscheid P, Economou IG, Leipertz A, Fröba AP. 2012 Viscosity, interfacial tension, self-diffusion coefficient, density, and refractive index of the ionic liquid 1-ethyl-3-methylimidazolium tetracyanoborate as a function of temperature at atmospheric pressure. *J. Chem. Eng. Data* **57**, 828–835. (doi:10.1021/je201080c)

193. Zhang QG, Yang JZ, Lu XM, Gui JS, Huang Z. 2004 Studies on an ionic liquid based on $FeCl_3$ and its properties. *Fluid Phase Equilib.* **226**, 207–211. (doi:10.1016/j.fluid.2004.09.020)
194. Součková M, Klomfar J, Pátek J. 2012 Temperature dependence of the surface tension and 0.1 MPa density for 1-C-n-3-methylimidazolium tris(pentafluoroethyl)trifluorophosphate with n = 2, 4, and 6. *J. Chem. Thermodyn.* **48**, 267–275. (doi:10.1016/j.jct.2011.12.033)
195. Jacquemin J, Ge R, Nancarrow P, Rooney DW, Costa Gomes MF, Pádua AAH, Hardacre C. 2008 Prediction of ionic liquid properties. I. Volumetric properties as a function of temperature at 0.1 MPa. *J. Chem. Eng. Data* **53**, 716–726. (doi:10.1021/je700707y)
196. Izgorodina EI, Golze D, Maganti R, Armel V, Taige M, Schubert TJS, MacFarlane DR. 2014 Importance of dispersion forces for prediction of thermodynamic and transport properties of some common ionic liquids. *Phys. Chem. Chem. Phys.* **16**, 7209–7221. (doi:10.1039/c3cp53035c)
197. Hunt PA, Gould IR, Kirchner B. 2007 The structure of imidazolium-based ionic liquids: insights from ion-pair interactions. *Aust. J. Chem.* **60**, 9–14. (doi:10.1071/CH06301)
198. Acree W, Chickos JS. 2016 Phase transition enthalpy measurements of organic and organometallic compounds. Sublimation, vaporization and fusion enthalpies from 1880 to 2015. Part 1. C_1–C_{10}. *J. Phys. Chem. Ref. Data* **45**, 565. (doi:10.1063/1.4948363)
199. Canongia Lopes JN, Pádua AAH. 2012 CL&P: a generic and systematic force field for ionic liquids modeling. *Theor. Chem. Acc.* **131**, 1129. (doi:10.1007/s00214-012-1129-7)
200. Marciniak A. 2010 The solubility parameters of ionic liquids. *Int. J. Mol. Sci.* **11**, 1973–1990. (doi:10.3390/ijms11051973)
201. Marciniak A. 2011 The Hildebrand solubility parameters of ionic liquids—part 2. *Int. J. Mol. Sci.* **12**, 3553–3575. (doi:10.3390/ijms12063553)
202. Marcus Y. 2017 Room temperature ionic liquids: their cohesive energies, solubility parameters and solubilities in them. *J. Solut. Chem.* **46**, 1778–1791. (doi:10.1007/s10953-10017-10634-10957)
203. Marcus Y. 2016 Are solubility parameters relevant for the solubility of liquid organic solutes in room temperature ionic liquids? *J. Mol. Liq.* **214**, 32–36. (doi:10.1016/j.molliq.2015.11.019)
204. Preiss UPRM, Slattery JM, Krossing I. 2009 *In Silico* prediction of molecular volumes, heat capacities, and temperature-dependent densities of ionic liquids. *Ind. Eng. Chem. Res.* **48**, 2290–2296. (doi:10.1021/ie801268a)
205. Tariq M, Freire MG, Saramago B, Coutinho JAP, Canongia Lopes JN, Rebelo LPN. 2012 Surface tension of ionic liquids and ionic liquid solutions. *Chem. Soc. Rev.* **41**, 829–868. (doi:10.1039/c1cs15146k)
206. Villar-Garcia IJ, Fearn S, De Gregorio GF, Ismail NL, Gschwend FJV, McIntosh AJS, Lovelock KRJ. 2014 The ionic liquid-vacuum outer atomic surface: a low-energy ion scattering study. *Chem. Sci.* **5**, 4404–4418. (doi:10.1039/c4sc00640b)
207. Santos CS, Baldelli S. 2009 Alkyl chain interaction at the surface of room temperature ionic liquids: systematic variation of alkyl chain length (R = C_1—C_4, C_8) in both cation and anion of [RMIM][R—OSO_3] by sum frequency generation and surface tension. *J. Phys. Chem. B* **113**, 923–933. (doi:10.1021/jp807924g)
208. Domanska U, Pobudkowska A, Rogalski M. 2008 Surface tension of binary mixtures of imidazolium and ammonium based ionic liquids with alcohols, or water: cation, anion effect. *J. Colloid Interface Sci.* **322**, 342–350. (doi:10.1016/j.jcis.2008.02.039)
209. Kőrösi G, Kováts ES. 1981 Density and surface-tension of 83 organic liquids. *J. Chem. Eng. Data* **26**, 323–332. (doi:10.1021/je00025a032)
210. Greaves TL, Weerawardena A, Drummond CJ. 2011 Nanostructure and amphiphile self-assembly in polar molecular solvents: amides and the 'solvophobic effect'. *Phys. Chem. Chem. Phys.* **13**, 9180–9186. (doi:10.1039/c1cp20481e)
211. Rolo LI, Caco AI, Queimada AJ, Marrucho IM, Coutinho JAP. 2002 Surface tension of heptane, decane, hexadecane, eicosane, and some of their binary mixtures. *J. Chem. Eng. Data* **47**, 1442–1445. (doi:10.1021/je025536+)
212. Marcus Y. 2017 Relationships between the internal pressure, the cohesive energy, and the surface tension of liquids. *Phys. Chem. Liq.* **55**, 522–531. (doi:10.1080/00319104.2016.1230739)
213. Santos CS, Baldelli S. 2010 Gas-liquid interface of room-temperature ionic liquids. *Chem. Soc. Rev.* **39**, 2136–2145. (doi:10.1039/b921580h)
214. Lovelock KRJ. 2012 Influence of the ionic liquid/gas surface on ionic liquid chemistry. *Phys. Chem. Chem. Phys.* **14**, 5071–5089. (doi:10.1039/c2cp23851a)
215. Mutelet F, Jaubert JN. 2007 Measurement of activity coefficients at infinite dilution in 1-hexadecyl-3-methylimidazolium tetrafluoroborate ionic liquid. *J. Chem. Thermodyn.* **39**, 1144–1150. (doi:10.1016/j.jct.2007.01.004)
216. Revelli AL, Mutelet F, Jaubert JN. 2009 Partition coefficients of organic compounds in new imidazolium based ionic liquids using inverse gas chromatography. *J. Chromatogr. A* **1216**, 4775–4786. (doi:10.1016/j.chroma.2009.04.004)
217. Foco GM, Bottini SB, Quezada N, de la Fuente JC, Peters CJ. 2006 Activity coefficients at infinite dilution in 1-alkyl-3-methylimidazolium tetrafluoroborate ionic liquids. *J. Chem. Eng. Data* **51**, 1088–1091. (doi:10.1021/je050544m)
218. Batista MLS, Neves CMSS, Carvalho PJ, Gani R, Coutinho JAP. 2011 Chameleonic behavior of ionic liquids and its impact on the estimation of solubility parameters. *J. Phys. Chem. B* **115**, 12 879–12 888. (doi:10.1021/jp207369g)
219. Jarvas G, Quellet C, Dallos A. 2011 Estimation of Hansen solubility parameters using multivariate nonlinear QSPR modeling with COSMO screening charge density moments. *Fluid Phase Equilib.* **309**, 8–14. (doi:10.1016/j.fluid.2011.06.030)
220. Mora-Pale M, Meli L, Doherty TV, Linhardt RJ, Dordick JS. 2011 Room temperature ionic liquids as emerging solvents for the pretreatment of lignocellulosic biomass. *Biotechnol. Bioeng.* **108**, 1229–1245. (doi:10.1002/bit.23108)
221. Weerachanchai P, Wong YW, Lim KH, Tan TTY, Lee JM. 2014 Determination of solubility parameters of ionic liquids and ionic liquid/solvent mixtures from intrinsic viscosity. *Chemphyschem* **15**, 3580–3591. (doi:10.1002/cphc.201402345)
222. Hernández-Bravo R, Miranda AD, Martínez-Mora O, Domínguez Z, Martínez-Magadán JM, García-Chávez R, Domínguez-Esquivel JM. 2017 Calculation of the solubility parameter by COSMO-RS methods and its influence on asphaltene-ionic liquid interactions. *Ind. Eng. Chem. Res.* **56**, 5107–5115. (doi:10.1021/acs.iecr.6b05035)
223. Moganty SS, Baltus RE. 2010 Regular solution theory for low pressure carbon dioxide solubility in room temperature ionic liquids: ionic liquid solubility parameter from activation energy of viscosity. *Ind. Eng. Chem. Res.* **49**, 5846–5853. (doi:10.1021/ie901837k)
224. Borodin O. 2009 Relation between heat of vaporization, ion transport, molar volume, and cation-anion binding energy for ionic liquids. *J. Phys. Chem. B* **113**, 12 353–12 357. (doi:10.1021/jp9070357)
225. Lee SH, Lee SB. 2005 The Hildebrand solubility parameters, cohesive energy densities and internal energies of 1-alkyl-3-methylimidazolium-based room temperature ionic liquids. *Chem. Commun.* **2005**, 3469–3471. (doi:10.1039/B503740A)
226. Weerachanchai P, Chen ZJ, Leong SSJ, Chang MW, Lee JM. 2012 Hildebrand solubility parameters of ionic liquids: effects of ionic liquid type, temperature and DMA fraction in ionic liquid. *Chem. Eng. J.* **213**, 356–362. (doi:10.1016/j.cej.2012.10.012)
227. Wong YW, Chen ZJ, Tan TTY, Lee JM. 2015 Hildebrand solubility parameters of amidium ionic liquids. *Ind. Eng. Chem. Res.* **54**, 12 150–12 155. (doi:10.1021/acs.iecr.5b02705)
228. Bonsa AM, Paschek D, Zaitsau DH, Emel'yanenko VN, Verevkin SP, Ludwig R. 2017 The relation between vaporization enthalpies and viscosities: eyring's theory applied to selected ionic liquids. *Chemphyschem.* **18**, 1242–1246. (doi:10.1002/cphc.201700138)
229. Marcus Y. 2010 The cohesive energy of molten salts and its density. *J. Chem. Thermodyn.* **42**, 60–64. (doi:10.1016/j.jct.2009.07.004)
230. Malberg F, Hollóczki O, Thomas M, Kirchner B. 2015 En route formation of ion pairs at the ionic liquid-vacuum interface. *Struct. Chem.* **26**, 1343–1349. (doi:10.1007/s11224-015-0662-0)
231. Safarov J, El-Awady WA, Shahverdiyev A, Hassel E. 2011 Thermodynamic properties of 1-ethyl-3-methylimidazolium bis(trifluoromethylsulfonyl)imide. *J. Chem. Eng. Data* **56**, 106–112. (doi:10.1021/je100945u)
232. Marcus Y. 2017 The internal pressure and cohesive energy density of liquid metallic elements. *Int. J. Thermophys.* **38**, 9. (doi:10.1007/s10765-016-2158-6)